

# Constraining lepton flavor violating $2q2\ell$ operators from low-energy cLFV processes

Utpal Chattopadhyay,<sup>1,\*</sup> Debottam Das,<sup>2,3,†</sup> Rahul Puri,<sup>2,3,‡</sup> and Joydeep Roy<sup>1,§</sup>

<sup>1</sup>*School of Physical Sciences, Indian Association for the  
Cultivation of Science, Jadavpur, Kolkata 700032, India*

<sup>2</sup>*Institute of Physics, Sachivalaya Marg, Bhubaneswar, 751005, India*

<sup>3</sup>*Homi Bhabha National Institute, Training School Complex, Anushakti Nagar, Mumbai 400094, India*

(Dated: July 18, 2025)

Charged lepton flavour-violating (cLFV) processes, which are definite proof of new physics beyond the Standard Model, have remained elusive experimentally till now. Effective Field Theory (EFT) has been very useful in providing information about such new physics through the higher-dimensional operators. These operators respect SM gauge invariance, and they are suppressed by appropriate powers of the energy scale  $\Lambda$ . In regard to lepton flavour violating (LFV) processes, the Standard Model Effective Field Theory (SMEFT) is shown to be a useful tool for estimating any new physics effect at the scale  $\Lambda$ . It is worth noticing that a large class of cLFV processes involve both quarks and leptons and thus low-energy observables play a significant role in providing bounds on lepton-flavour-violating 2-quark-2-lepton ( $2q2\ell$ ) operators. Therefore, in this work, we have collected several low-energy cLFV processes that can be addressed within the SMEFT framework and also collected the set of operators responsible for such processes. Keeping in mind the correlation that exists among the SMEFT operators, we want to extract the strongest constraints on these  $2q2\ell$  operators.

---

\* [tpuc@iacs.res.in](mailto:tpuc@iacs.res.in)

† [debottam@iopb.res.in](mailto:debottam@iopb.res.in)

‡ [rahul.puri@iopb.res.in](mailto:rahul.puri@iopb.res.in)

§ [spsjr2729@iacs.res.in](mailto:spsjr2729@iacs.res.in); [joyroy.phy@gmail.com](mailto:joyroy.phy@gmail.com)

## I. Introduction

The Standard Model (SM) [1] has been extraordinarily successful in elucidating the fundamental interactions between constituent particles. It has made precise predictions that have been verified by experiments at accelerators such as LEP [2], Tevatron [3], and the LHC [4]. The discovery of the Higgs boson at the LHC in 2012 [5] was the last missing piece of the SM puzzle, and it firmly establishes the SM as the appropriate theory for the energy range we have explored. However, SM is still far from becoming a comprehensive account of particle physics [6]. There are several experimental facts and theoretical questions that cannot be addressed by staying within the SM framework. These include the gauge hierarchy problem, the mass of neutrinos, the lack of a particle dark matter (DM) candidate, and the baryon asymmetry of the universe, among other significant problems that drive our investigation of physics Beyond the SM (BSM) scenarios. Direct and indirect avenues exist for exploring the potential existence of New Physics (NP). Direct approaches involve detecting new particles through ongoing and upcoming collider experiments, while indirect probes rely on evidence gathered from various low-energy processes. Among many potential BSM signals, charged lepton flavour violation stands out as an intriguing and promising candidate for investigating NP scenarios. It is known that flavour-changing neutral current (FCNC) processes can be substantially large in many BSM scenarios. In contrast, they are heavily suppressed in the SM by small Cabibbo-Kobayashi-Maskawa (CKM) matrix elements, loop effects, etc. Probing NP models with FCNC effects can thus be quite useful. Such effects can be seen in several cLFV processes, which are tabulated in Table-I with their current experimental upper limits.

In the model-dependent category, various popular models have been used to accommodate cLFV processes, but to date, searches at the LHC have not yielded any direct evidence of a new particle. Strong arguments in support of BSM physics and these null results can become the motivation for considering an Effective Field Theory (EFT) approach [7?–9] to estimate the level of unknown physics interactions at a given scale. In contrast to considering a BSM model that is associated with a top-down approach to an EFT framework, one can adopt a bottom-up approach [9? ] and here, this refers to the model-independent investigation within the Standard Model Effective Field Theory (SMEFT) [8?–10] where the energy scale  $\Lambda$  of effective interactions can be above the reach of current experiments. In SMEFT, one considers higher-dimensional effective local operators out of SM fields only. The operators respect SM gauge invariance, and they are suppressed by appropriate powers of  $\Lambda$ . In regard to LFV processes, SMEFT is shown to be a useful tool for estimating any new physics effect at the scale  $\Lambda$  [11–18].

For example, SMEFT has been used to study general LFV processes [12, 19, 20], LFV  $B$ -meson decays (LFVBDs) [21–26], Z boson LFV decays (ZLFVDs) [27], Higgs boson LFV decays (HLFVDs) [28] or LFV Quarkonium decays (LFVQDs) [29]. Although these references are hardly an exhaustive list of such works, it has been shown in all of them that the most dominant contributions to LFV processes come from dimension-6 operators, and the operators contributing to leptonic or semi-leptonic processes are either of the Higgs-fermion or four-fermion type. But for our present purpose, we focus our attention on the inputs from low-energy precision experiments as they are particularly sensitive to NP. In this regard, a subset of dimension-6 four-fermion operators involving two quarks and two leptons is particularly relevant. Specifically, these operators with different lepton flavours contribute to a wide range of low-energy LFV observables that are experimentally accessible. We shall refer to them as LFV  $2q2\ell$  operators hereafter in this paper and estimate the bounds on them by comparing low-energy observables dependent on them. A comprehensive list of these operators within the SMEFT framework, with their chirality structure, is given in Table-II while a similar list of effective operators appropriate for low-energy is provided in Table-III.

Several studies have compiled constraints on four-fermionic operators [72–76]. However, in all

Observables of cLFV modes.	Present bounds		Expected future limits		Flavio
$BR(\tau \rightarrow e\pi^0)$	$8.0 \times 10^{-8}$	Belle(2007) [30]	$7.3 \times 10^{-10}$	Belle-II[31]	✓
$BR(\tau \rightarrow \mu\pi^0)$	$1.1 \times 10^{-7}$	BaBar(2006) [32]	$(5 \times 10^{-10})$ $7.1 \times 10^{-10}$	Belle-II[31, 33]	✓
$BR(\tau \rightarrow e\rho^0)$	$2.2 \times 10^{-8}$	Belle(2023) [34]	$3.8 \times 10^{-10}$	Belle-II[33]	✓
$BR(\tau \rightarrow \mu\rho^0)$	$1.7 \times 10^{-8}$	Belle(2023) [34]	$5.5 \times 10^{-10}$	Belle-II[33]	✓
$BR(\tau \rightarrow e\phi)$	$2.0 \times 10^{-8}$	Belle(2023) [34]	$7.4 \times 10^{-10}$	Belle-II[33]	✓
$BR(\tau \rightarrow \mu\phi)$	$2.3 \times 10^{-8}$	Belle(2023) [34]	$8.4 \times 10^{-10}$	Belle-II[33]	✓
$BR(\tau \rightarrow e(\mu)K_S^0)$	$0.8(1.2) \times 10^{-8}$	Belle-II(2025) [35]			✓✓
$CR(\mu - e, Au)$	$7.0 \times 10^{-13}$	SINDRUMII(2006) [36]	-	-	✓
$CR(\mu - e, Ti)$	$6.1 \times 10^{-13}$	SINDRUMII(1998)[37]	-	-	✓
$CR(\mu - e, Al)$	-	-	$10^{-17}$	Mu2e[38]	✓
	-	-	$10^{-15}$ (Phase I) & $10^{-17}$ (Phase II)	COMET at J-PARC[39, 40]	✓
$BR(J/\Psi \rightarrow e^\pm\mu^\mp)$	$4.5 \times 10^{-9}$	BESIII(2022) [41]			✓
$BR(J/\Psi \rightarrow e\tau)$	$7.5 \times 10^{-8}$	BESIII(2021) [42]			✓
$BR(J/\Psi \rightarrow \mu\tau)$	$2.0 \times 10^{-6}$	BES(2004) [43]			✓
$BR(\Upsilon(1S) \rightarrow e\mu)$	$3.9 \times 10^{-7}$	Belle(2022) [44]			✓
$BR(\Upsilon(1S) \rightarrow e\tau)$	$2.7 \times 10^{-6}$	Belle(2022) [44]			✓
$BR(\Upsilon(1S) \rightarrow \mu\tau)$	$2.7 \times 10^{-6}$	Belle(2022) [44]			✓
$BR(\Upsilon(2S) \rightarrow e\tau)$	$1.12 \times 10^{-6}$	Belle(2024) [45]			✓
$BR(\Upsilon(2S) \rightarrow \mu\tau)$	$2.3 \times 10^{-7}$	Belle(2024) [45]			✓
$BR(\Upsilon(3S) \rightarrow e\mu)$	$3.6 \times 10^{-7}$	BaBar(2022) [46]			✓
$BR(\Upsilon(3S) \rightarrow e\tau)$	$4.2 \times 10^{-6}$	BaBar(2010) [47]			✓
$BR(\Upsilon(3S) \rightarrow \mu\tau)$	$3.1 \times 10^{-6}$	BaBar(2010) [47]			✓
$BR(\pi^0 \rightarrow e^\pm\mu^\mp)$	$3.2 \times 10^{-10}$	NA62(2021) [48]	-	-	✓✓
$BR(\pi^0 \rightarrow e^\pm\mu^\mp)$	$3.8 \times 10^{-10}$	SPEC(2000) [49]	-	-	✓✓
$BR(\pi^0 \rightarrow e^\pm\mu^\mp)$	$3.6 \times 10^{-10}$	KTeV(2007) [50]	-	-	✓✓
$BR(\eta^0 \rightarrow e\mu)$	$6.0 \times 10^{-6}$	SPES2(1995) [51]			✓
$BR(\eta^{0\prime} \rightarrow e\mu)$	$4.7 \times 10^{-4}$	CLEO II(1999) [52]	JEF [? ], REDTOP [53]		✓✓
$BR(K_L^0 \rightarrow e^\pm\mu^\mp)$	$4.7 \times 10^{-12}$	BNL E871(1998) [54]			✓
$BR(K_L \rightarrow \pi^0 e\mu)$	$7.6 \times 10^{-11}$	KTeV(2008) [50]	-	-	✓✓
$BR(K^+ \rightarrow \pi^+\mu^-e^+)$	$6.6 \times 10^{-11}$	NA62(2021) [48]			✓✓
$BR(K^+ \rightarrow \pi^+\mu^+e^-)$	$1.3 \times 10^{-11}$	E865(2005) [55]			✓✓
$BR(D^0 \rightarrow e^\pm\mu^\mp)$	$1.3 \times 10^{-8}$	LHCb(2016) [56]			✓✓
$BR(D^0 \rightarrow \pi^0 e^\pm\mu^\mp)$	$8 \times 10^{-7}$	BaBar(2020) [57]			×
$BR(D^0 \rightarrow \rho^0(\phi)e^\pm\mu^\mp)$	$5(5.1) \times 10^{-7}$	BaBar(2020) [57]			×
$BR(D^0 \rightarrow \omega e^\pm\mu^\mp)$	$17.1 \times 10^{-7}$	BaBar(2020) [57]			×
$BR(D^0 \rightarrow \eta e^\pm\mu^\mp)$	$22.5 \times 10^{-7}$	BaBar(2020) [57]			×
$BR(D^+ \rightarrow \pi^+e^{+(-)}\mu^{-(+)})$	$2.1(2.2) \times 10^{-7}$	LHCb(2020) [58]			✓✓
$BR(D_s^+ \rightarrow K^+e^{+(-)}\mu^{-(+)})$	$1.4 \times 10^{-8} - 6.4 \times 10^{-6}$	LHCb(2020) [58]			✓✓
$BR(B^+ \rightarrow K^+e^{+(-)}\mu^{-(+)})$	$7.0(6.4) \times 10^{-9}$	LHCb(2019) [59]	-	-	✓
$BR(B^0 \rightarrow K^{*0}e^{+(-)}\mu^{-(+)})$	$6.8(5.7) \times 10^{-9}$	LHCb(2022) [60]	-	-	✓
$BR(B^0 \rightarrow \pi^0 e^\pm\mu^\mp)$	$1.4 \times 10^{-7}$	BaBar(2007) [61]	-	-	✓
$BR(B^+ \rightarrow \pi^+ e^\pm\mu^\mp)$	$1.7 \times 10^{-7}$	BaBar(2007) [61]	-	-	✓
$BR(B_s^0 \rightarrow \phi\mu^\pm e^\mp)$	$16 \times 10^{-9}$	LHCb(2022) [60]	-	-	✓
$BR(B_s^0 \rightarrow \mu^\mp e^\pm)$	$5.4 \times 10^{-9}$	LHCb(2018) [62]	$3 \times 10^{-10}$	LHCb-II [63]	✓
$BR(B^0 \rightarrow \mu^\mp e^\pm)$	$1.0 \times 10^{-9}$	LHCb(2018) [62]	$3 \times 10^{-10}$	LHCb-II [63]	✓
$BR(B^+ \rightarrow K^+\mu^{-(+)}\tau^{(-)})$	$0.59(2.45) \times 10^{-5}$	Belle(2022) [64]	$3.3 \times 10^{-6}$	Belle-II [33]	✓
$BR(B^+ \rightarrow K^+e^{+(-)}\tau^{-(+)})$	$1.53(1.51) \times 10^{-5}$	Belle(2022) [64]	$2.1 \times 10^{-6}$	Belle-II [33]	✓
$BR(B^0 \rightarrow K^{*0}\mu^{+(-)}\tau^{-(+)})$	$8.2(10) \times 10^{-6}$	LHCb(2022) [65]	-	-	✓
$BR(B^+ \rightarrow \pi^+e^{+(-)}\tau^{-(+)})$	$7.4(2.0) \times 10^{-5}$	BaBar(2012) [66]	-	-	✓
$BR(B^+ \rightarrow \pi^+\mu^{+(-)}\tau^{-(+)})$	$6.2(4.5) \times 10^{-5}$	BaBar(2012) [66]	-	-	✓
$BR(B_s^0 \rightarrow \phi\mu^\pm\tau^\mp)$	$1.0 \times 10^{-5}$	LHCb(2024) [67]	-	-	✓
$BR(B^0 \rightarrow \tau^\pm e^\mp)$	$1.6 \times 10^{-5}$	Belle(2021) [68]	-	-	✓
$BR(B^0 \rightarrow \tau^\pm\mu^\mp)$	$1.2 \times 10^{-5}$	LHCb(2019) [69]	$1.3 \times 10^{-6}$	Belle-II [33]	✓
$BR(B_s^0 \rightarrow \tau^\pm e^\mp)$	$1.4 \times 10^{-3}$	Belle(2023) [70]	-	-	✓
$BR(B_s^0 \rightarrow \tau^\pm\mu^\mp)$	$3.4 \times 10^{-5}$	LHCb(2019) [69]	-	-	✓

TABLE I: Present upper bounds (with 90% CL), and future expected sensitivities of branching ratios for the set of low-energy cLFV transitions relevant for our analysis.  $K_L^0 \rightarrow (e/\mu)^\pm\tau^\mp$  decay modes are forbidden by phase space. Similar for the mode  $D^0 \rightarrow \mu^\pm\tau^\mp$  [71]. The last column represents whether the Python codes for the corresponding LFV processes are available in the Flavio package or not. A regular ‘✓’ means it is already implemented, and a bold ‘✓✓’ means it is implemented by us for the first time for this analysis. ‘×’ sign represents an observable which is neither available in Flavio nor implemented by us.<sup>a</sup>

<sup>a</sup> We plan to implement a few other LFV processes, such as  $\tau^\pm \rightarrow (e/\mu)^\pm\omega$  or  $D^0 \rightarrow (\omega/\rho^0)e^\pm\mu^\mp$  etc., that are not implemented in flavio, in our future analysis.

of these works, the analysis was either limited to a subset of the  $2q2\ell$  operators or conducted

in terms of the WCs with broad Lorentz structures—vector, axial-vector, tensor, or pseudoscalar—without distinguishing between specific flavour indices. But here we try to impose constraints only on LFV  $2q2\ell$  operators with specific quark and lepton indices, which are responsible for specific LFV processes. Based on the involvement of quarks and leptons in each process and corresponding EFT analysis, Table-IV presents a set of LFV  $2q2\ell$  operators that contribute dominantly to those processes.<sup>1</sup> Furthermore, in Table-V we tabulate all mesons considered in this analysis and their quark compositions, whereas Tables-VI-VII have been used for representing relevant data used.

These operators contribute to the LFV processes in two possible scenarios. First, where processes involve different quark-flavour transitions, like decays of pseudoscalar mesons ( $B, K, D$ ), as described in Table-IX. Second, where the system involves the same quark flavour like quarkonium ( $q\bar{q}$ ) or  $\tau$  decaying to vector and pseudoscalar mesons, as described in Tables-X and XI. Moreover, these operators have important phenomenological consequences because several bosonic mediators, such as a second Higgs doublet, vector bosons, various low-energy scalar or leptoquark models [77–80] can induce them.

In most SMEFT analyses, a common simplification is to consider only one operator at a time, with others being zero. Although this single-operator setup is not ideal for a realistic low-energy description of any UV-completion scenario, such analysis provides very useful information about the new physics scale  $\Lambda$  that can be probed if that operator exists at that scale. Moreover, when several observables, all of which are dependent on a specific operator, are considered, the single-operator method provides a way to perform the sensitivity test among those observables. As we shall explain in this paper, the information from such a test helps identify which observables are most relevant to constrain a particular operator, assuming it is generated by some underlying UV model. The third important aspect of this so-called ‘1-d analysis’ comes from the fact that several of these LFV  $2q2\ell$  operators ( $\mathcal{C}_{\ell q}^{(1)}, \mathcal{C}_{\ell q}^{(3)}$  and  $\mathcal{C}_{qe}$ ) are important in imposing constraints on other LFVs such as ZLFV or 3-body leptonic decays [27] through the Higgs-lepton operators ( $\mathcal{C}_{\phi\ell}^{(1)}, \mathcal{C}_{\phi\ell}^{(3)}, \mathcal{C}_{\phi e}$ ), as they are strongly related via RGEs. Moreover, several of these LFV operators can be related to other non-LFV processes as well and thus signifying the phenomenological relevance of the constraints obtained from this analysis.

We also performed analysis beyond this simplistic approach by considering the simultaneous presence of two operators at the UV scale and presented some of those results. In sec-II we provide a general effective field theory framework and a comprehensive list of dim-6 operators responsible for LFV processes. There, we also discuss the procedure and methods used to match the SMEFT and LEFT operator basis. All relevant expressions for our analysis are presented in terms of SMEFT operators in sec-III. In this analysis, for the first time, we have implemented several LFV decay modes through *Flavio*. Form factors and other necessary elements needed to write those codes are presented in Tables-VII-VIII in sec-IV. Results of this analysis are presented in section V, and finally we conclude in sec-VII.

## II. Standard Model Effective Field Theory Framework

New physics involving heavy particles may be present at scales ( $\Lambda$ ) beyond the current experimental reach. To study its effects on the interactions of SM fields between  $\Lambda$  and the EW-scale in a model-independent way, higher-dimensional operators involving the SM fields only can be proposed. This effective description is called the SMEFT. The operators are suppressed by appropriate powers of  $\Lambda$  ( $\gg m_W$ ) and corresponding Wilson coefficients (WCs) parameterise the low-energy behaviour of such high-energy theory through the running of the renormalisation group equations.

<sup>1</sup> We do not consider the high-energy LFV processes involving bosons (Higgs or  $Z$ ) or 3-body decays of leptons in this analysis or the processes where these operators can be produced in the loop, e.g. LFVZ decays.

(RGEs) of masses and coupling parameters of the theory. The SMEFT Lagrangian is given by [9, 10]

$$\mathcal{L}_{\text{SMEFT}} = \mathcal{L}_{\text{SM}} + \frac{1}{\Lambda} \mathcal{C}^{(5)} \mathcal{O}^{(5)} + \frac{1}{\Lambda^2} \sum_n \mathcal{C}_n^{(6)} \mathcal{O}_n^{(6)} + \mathcal{O}\left(\frac{1}{\Lambda^3}\right) + \dots \quad (1)$$

where  $\mathcal{L}_{\text{SM}}$  is the usual renormalizable SM Lagrangian,  $\mathcal{O}^{(5)}$  represents the gauge-invariant mass dimension-5 operators, known as neutrino mass generating Weinberg operator,  $\mathcal{C}^{(5)}$  is the corresponding WCs. Similarly,  $\mathcal{O}_n^{(6)}$  and  $\mathcal{C}_n^{(6)}$  represent mass dimension-6 operators and corresponding WCs respectively. In this work, we will not consider any more terms with suppression level greater than  $1/\Lambda^2$ .

2-quark-2-lepton operators			
Vector	$[\mathcal{O}_{\ell q}^{(1)}]_{\alpha\beta ij}$	$(\bar{L}_\alpha \gamma_\mu L_\beta)(\bar{Q}_i \gamma^\mu Q_j)$	$(\bar{L}L)(\bar{L}L)$
	$[\mathcal{O}_{\ell q}^{(3)}]_{\alpha\beta ij}$	$(\bar{L}_\alpha \gamma_\mu \tau^I L_\beta)(\bar{Q}_i \gamma^\mu \tau^I Q_j)$	$(\bar{L}L)(\bar{L}L)$
	$[\mathcal{O}_{qe}]_{ij\alpha\beta}$	$(\bar{Q}_i \gamma_\mu Q_j)(\bar{E}_\alpha \gamma^\mu E_\beta)$	$(\bar{L}L)(\bar{R}R)$
	$[\mathcal{O}_{\ell d}]_{\alpha\beta ij}$	$(\bar{L}_\alpha \gamma_\mu L_\beta)(\bar{D}_i \gamma^\mu D_j)$	$(\bar{L}L)(\bar{R}R)$
	$[\mathcal{O}_{\ell u}]_{\alpha\beta ij}$	$(\bar{L}_\alpha \gamma_\mu L_\beta)(\bar{U}_i \gamma^\mu U_j)$	$(\bar{L}L)(\bar{R}R)$
	$[\mathcal{O}_{ed}]_{\alpha\beta ij}$	$(\bar{E}_\alpha \gamma_\mu E_\beta)(\bar{D}_i \gamma^\mu D_j)$	$(\bar{R}R)(\bar{R}R)$
	$[\mathcal{O}_{eu}]_{\alpha\beta ij}$	$(\bar{E}_\alpha \gamma_\mu E_\beta)(\bar{U}_i \gamma^\mu U_j)$	$(\bar{R}R)(\bar{R}R)$
Scalar	$[\mathcal{O}_{\ell edq}]_{\alpha\beta ij}$	$(\bar{L}_\alpha^a E_\beta)(\bar{D}_i Q_j^a)$	$(\bar{L}R)(\bar{R}L)$
	$[\mathcal{O}_{\ell equ}^{(1)}]_{\alpha\beta ij}$	$(\bar{L}_\alpha^a E_\beta) \epsilon_{ab} (\bar{Q}_i^b U_j)$	$(\bar{L}R)(\bar{L}R)$
Tensor	$[\mathcal{O}_{\ell equ}^{(3)}]_{\alpha\beta ij}$	$(\bar{L}_\alpha^a \sigma_{\mu\nu} E_\beta) \epsilon_{ab} (\bar{Q}_i^b \sigma^{\mu\nu} U_j)$	$(\bar{L}R)(\bar{L}R)$

TABLE II: A comprehensive list of dimension-6  $2q2\ell$  operators that remain invariant under the SM gauge group and contribute to LFV observables. In these expressions,  $Q$  and  $L$  represent left-handed quark and lepton  $SU(2)$  doublets, respectively, with indices  $a, b = 1, 2$ .  $U$ ,  $D$  and  $E$  denote right-handed up, down quark and lepton singlets. The last column provides the chirality of fermionic currents of these operators.

In general studies of low-energy observables in SMEFT, there are three energy scales. A high energy scale  $\Lambda$ , an intermediate energy scale of electroweak symmetry-breaking  $m_{Z/W}$  and a low-energy scale like  $\sim m_b$  or  $m_{\tau/\mu}$ . Therefore for probing the level of contributions of the higher dimensional operators for LFV studies that may be consistent with experimental constraints, a general method of “match and run” of RGEs is described below. At the first step, the SMEFT 1-loop RGEs [81–83] of relevant WCs would be initialised at the scale  $\Lambda$  ( $\sim \text{TeV}$ ) and run down to the electroweak scale  $\sim m_{Z/W}$ . The WCs under study are given a non-vanishing value like unity, while other WCs are set to zero at the scale  $\Lambda$  and RGE evolution is completed till the electroweak scale  $m_{Z/W}$ . Of course, the WCs are hardly expected to remain at their initial values, including also the ones that were vanishing at the high scale  $\Lambda$ . This level of evolution is adequate for the LFV decays of the  $t$ ,  $Z$  or Higgs bosons but not enough for processes referring to energies below the electroweak scale. Further down the scale, in the second step, as in a top-down approach of EFT, the heavy particles of the theory ( $W^\pm$ ,  $Z$ , the Higgs boson and the top quark) are integrated out and the operators invariant under the  $\text{QCD} \times \text{QED}$  gauge groups and consisting of fields of light charged fermions ( $u, d, c, s, b, e, \mu, \tau$ ), neutral fermions ( $\nu_e, \nu_\mu, \nu_\tau$ ) and massless gauge bosons describe the effective interactions. These operators are known as Low-energy Effective Field Theory

(LEFT) operators that contribute to the total LEFT Lagrangian containing dimension three and higher dimensional ( $d > 4$ ) operators. Most general interacting Lagrangian can be written as:

$$\mathcal{L}_{\text{LEFT}}^{(\text{int})} = -\mathcal{H}_{\text{eff}} = \sum_{O_i=O_i^\dagger} \frac{1}{v^2} C_i O_i + \sum_{O_i \neq O_i^\dagger} \frac{1}{v^2} (C_i O_i + \text{h.c.}). \quad (2)$$

where,  $v = (\sqrt{2}G_F)^{-1/2}$ ,  $G_F$  being the Fermi-constant. For our purpose the most relevant dimension-six LEFT operators are those containing four fermions, with one spinor bilinear involving charged leptons of different flavours and the other involving quarks [84]. Schematically, these operators take the form

$$\mathcal{O}_{eq}^{S,AB} = (\bar{e}_\alpha \Gamma_S P_A e_\beta) (\bar{q}_i \Gamma_S P_B q_j), \quad q \in \{u, d\} \quad (3)$$

where  $e, u$  and  $d$ , represents charged leptons, up-type quarks and down type quarks respectively. The indices  $(\alpha\beta)$  and  $(ij)$  represent the generations of the leptons and quarks respectively.  $P_{A,B}$  are the left and right projection operators and  $\Gamma_S \in \{\mathbb{1}, \gamma_\mu, \sigma_{\mu\nu}\}$  for scalar, vector and tensor respectively. All such operators, along with the leptonic dipole operators, with the corresponding WCs, are listed in Table-III.

	Wilson Coefficient ( $C$ )	Operator ( $O$ )
Vector	$(C_{eu}^{V,XY})_{\alpha\beta ij}$	$(\bar{e}_\alpha \gamma^\mu P_X e_\beta) (\bar{u}_i \gamma_\mu P_Y u_j)$
	$(C_{ed}^{V,XY})_{\alpha\beta ij}$	$(\bar{e}_\alpha \gamma^\mu P_X e_\beta) (\bar{d}_i \gamma_\mu P_Y d_j)$
Scalar	$(C_{eu}^{S,XY})_{\alpha\beta ij}$	$(\bar{e}_\alpha P_X e_\beta) (\bar{u}_i P_Y u_j)$
	$(C_{ed}^{S,XY})_{\alpha\beta ij}$	$(\bar{e}_\alpha P_X e_\beta) (\bar{d}_i P_Y d_j)$
Tensor	$(C_{eu}^{T,RR})_{\alpha\beta ij}$	$(\bar{e}_\alpha \sigma^{\mu\nu} P_R e_\beta) (\bar{u}_i \sigma_{\mu\nu} P_R u_j)$
	$(C_{ed}^{T,RR})_{\alpha\beta ij}$	$(\bar{e}_\alpha \sigma^{\mu\nu} P_R e_\beta) (\bar{d}_i \sigma_{\mu\nu} P_R d_j)$
Dipole	$(C_{e\gamma})_{\alpha\beta}$	$(\bar{e}_\alpha \sigma^{\mu\nu} P_R e_\beta) F_{\mu\nu}$

TABLE III:  $2q2\ell$  Wilson coefficients and the corresponding operators. Here,  $P_{X,Y}$  denote the chiral projection operators with  $X, Y \in \{L, R\}$ , and the indices  $\alpha, \beta, i, j \in \{1, 2, 3\}$  label fermion generations excluding the top-quark.

Following the “match and run” procedure, the LEFT WCs are matched at tree level to the SMEFT operators at the scale  $m_Z$ , which are given in Appendix A (for details, see Refs.[85, 86]). In the third and final step, these LEFT coefficients are evolved down to the relevant low-energy scale of the process under consideration ( $m_\tau, m_\mu$  or  $m_b$ ) to evaluate the desired experimental observables. We implement all these procedures in our numerical analysis with the help of the Wilson [87] and Flavio [88] packages.

#### Change of Basis in LEFT

Instead of chiral operators, the LEFT can also be expressed in terms of operators constructed from fermion currents classified by their Lorentz structure (LS), namely scalar ( $S$ ), pseudoscalar ( $P$ ), vector ( $V$ ), axial-vector ( $A$ ), tensor ( $T$ ), and pseudotensor ( $T5$ ). The leptonic dipole operators



can also be written as tensor-dipole ( $D$ ) and pseudotensor-dipole ( $D5$ ) as:

$$\begin{aligned} \mathcal{L}_{\text{LEFT}}^{(\text{int})} \supset & \frac{1}{4} \sum_{J,K} \frac{1}{v^2} C_{JK}^{\alpha\beta ij} \left( \bar{e}_\alpha \hat{G}_J e_\beta \right) \left( \bar{q}_i \hat{G}_K q_j \right) + \frac{1}{4} \sum_{M,N} \frac{1}{v^2} C_{MN}^{\alpha\beta ij} \left( \bar{e}_\alpha \hat{G}_M^\mu e_\beta \right) \left( \bar{q}_i (\hat{G}_N)_\mu q_j \right) \\ & + \frac{1}{2v^2} C_T^{\alpha\beta ij} (\bar{e}_\alpha \sigma^{\mu\nu} e_\beta) (\bar{q}_i \sigma_{\mu\nu} q_j) + \frac{1}{2v^2} C_{T5}^{\alpha\beta ij} (\bar{e}_\alpha \sigma^{\mu\nu} e_\beta) (\bar{q}_i \sigma_{\mu\nu} \gamma_5 q_j) \\ & + \frac{1}{2v^2} C_D^{\alpha\beta} (\bar{e}_\alpha \sigma^{\mu\nu} e_\beta) F_{\mu\nu} + \frac{1}{2v^2} C_{D5}^{\alpha\beta} (\bar{e}_\alpha \sigma^{\mu\nu} \gamma_5 e_\beta) F_{\mu\nu} \end{aligned} \quad (4)$$

where  $J, K \in \{S, P\}$  and  $M, N \in \{V, A\}$ . The matrices  $\hat{G}^{(\mu)}$  are defined as:

$$\hat{G}_S = \mathbb{1}, \quad \hat{G}_P = \gamma_5, \quad \hat{G}_V^\mu = \gamma^\mu, \quad \hat{G}_A^\mu = \gamma^\mu \gamma_5. \quad (5)$$

The transformation from the chiral WCs (Table-III) to the LS WCs is given by:

$$\begin{aligned} \begin{bmatrix} C_{VV} \\ C_{AV} \\ C_{VA} \\ C_{AA} \end{bmatrix} &= \begin{bmatrix} 1 & 1 & 1 & 1 \\ -1 & -1 & 1 & 1 \\ -1 & 1 & -1 & 1 \\ 1 & -1 & -1 & 1 \end{bmatrix} \begin{bmatrix} C^{V,LL} \\ C^{V,LR} \\ C^{V,RL} \\ C^{V,RR} \end{bmatrix}, \quad \begin{bmatrix} C_{SS} \\ C_{SP} \\ C_{PS} \\ C_{PP} \end{bmatrix} = \begin{bmatrix} 1 & 1 & 1 & 1 \\ -1 & -1 & 1 & 1 \\ -1 & 1 & -1 & 1 \\ 1 & -1 & -1 & 1 \end{bmatrix} \begin{bmatrix} C^{S,LL} \\ C^{S,LR} \\ C^{S,RL} \\ C^{S,RR} \end{bmatrix} \\ \begin{bmatrix} C_T^{\alpha\beta ij} \\ C_{T5}^{\alpha\beta ij} \end{bmatrix} &= \begin{bmatrix} 1 & 1 \\ -1 & 1 \end{bmatrix} \begin{bmatrix} (C^{T,RR})_{\beta\alpha ji}^* \\ (C^{T,RR})_{\alpha\beta ij} \end{bmatrix}, \quad \begin{bmatrix} C_D^{\alpha\beta} \\ C_{D5}^{\alpha\beta} \end{bmatrix} = \begin{bmatrix} 1 & 1 \\ -1 & 1 \end{bmatrix} \begin{bmatrix} C_{e\gamma}^{\beta\alpha*} \\ C_{e\gamma}^{\alpha\beta} \end{bmatrix} \end{aligned} \quad (6)$$

where, the lepton flavour indices ( $\alpha\beta$ ) and quark flavour indices ( $ij$ ) as well as the class of WCs ( $C_{eu}/C_{ed}$ ) are implicit unless specified.

### III. Observables & operators relevant for different LFV processes

All the processes considered in this analysis can be broadly classified into three categories based on the quark FCNC involved. The majority of the processes feature interactions through a  $d$ -type FCNC, while some involve a  $u$ -type FCNC. The remaining processes include interactions through both types of FCNCs. This classification by quark FCNC, together with the type of meson (vector or pseudoscalar), is critical in identifying the class of operators relevant to each process. Table-IV classifies the LFV processes that have experimental data along with corresponding classes of operators responsible for such processes.

These observables can further be classified based on the the initial and final states of the process, namely pure leptonic decays of pseudoscalar and vector mesons ( $\mathcal{P}/\mathcal{V} \rightarrow \ell_i \ell_j$ ), semileptonic decays of pseudoscalars ( $\mathcal{P} \rightarrow (\mathcal{P}'/\mathcal{V}) \ell_i \ell_j$ ),  $\tau$  decays to mesons ( $\tau \rightarrow (\mathcal{P}/\mathcal{V}) \ell$ ) and conversion of muon to electron at a nucleus ( $\mu N \rightarrow e N$ ). Below, we discuss briefly the general procedure to analyse these processes and then provide relevant general expressions for all of them in terms of LEFT WCs, which can be related to the SMEFT WCs through “*running and matching*”. The same can be identified based on the flavours of leptons and quarks involved in the process (see Tables-IX–XI).

#### A. LFV semi-leptonic decays of pseudoscalar ( $\mathcal{P}$ ) mesons

In this section, we shall discuss the LFV decays of pseudoscalar mesons, which are characterised by zero spin and odd parity. This class of mesons can further be categorised into two segments. A meson *nonet*, consisting of light quarks ( $u, d$  and  $s$ ) such as pion ( $\pi$ ), eta ( $\eta$ ), eta prime ( $\eta'$ )

Interacting quark type	Meson type	Process	Energy scale ( $\mu$ )	Relevant classes for $2q2\ell$ Operators			
$d$ -type ( $d, s, b$ )	$\mathcal{P}$	$K_L^0 \rightarrow \ell_1 \ell_2$ $K_L^0 \rightarrow \pi^0 \ell_1 \ell_2$ $K^\pm \rightarrow \pi^\pm \ell_1 \ell_2$	500 MeV	$\mathcal{O}_{\ell q}^{(1)}, \mathcal{O}_{\ell q}^{(3)}, \mathcal{O}_{qe}, \mathcal{O}_{ed}, \mathcal{O}_{ld}, \mathcal{O}_{ledq}$			
		$B^0 \rightarrow \ell_1 \ell_2$ $B^{0(\pm)} \rightarrow \pi^{0(\pm)} \ell_1 \ell_2$ $B^{0(\pm)} \rightarrow K^{*0(\pm)} \ell_1 \ell_2$ $B_s^0 \rightarrow \ell_1 \ell_2$ $B_s^0 \rightarrow \phi^0 \ell_1 \ell_2$	5 GeV				
		$\tau^\pm \rightarrow K_S \ell^\pm$	2 GeV				
		$\mathcal{V}$	$\tau^\pm \rightarrow \phi^0 \ell^\pm$		2 GeV	$\mathcal{O}_{\ell q}^{(1)}, \mathcal{O}_{\ell q}^{(3)}, \mathcal{O}_{qe}, \mathcal{O}_{ed}, \mathcal{O}_{ld}$	
			$\Upsilon \rightarrow \ell_1 \ell_2$		10 GeV		
		$u$ -type ( $u, c$ )	$\mathcal{P}$		$D^0 \rightarrow \mu^\pm e^\mp$ $D^{0(\pm)} \rightarrow \pi^{0(\pm)} \mu^\pm e^\mp$ $D_s^\pm \rightarrow K^\pm \mu^\pm e^\mp$	2 GeV	$\mathcal{O}_{\ell q}^{(1)}, \mathcal{O}_{\ell q}^{(3)}, \mathcal{O}_{qe}, \mathcal{O}_{eu}, \mathcal{O}_{lu}, \mathcal{O}_{lequ}^{(1)}, \mathcal{O}_{lequ}^{(3)}$
					$\mathcal{V}$	$J/\psi \rightarrow \ell_1 \ell_2$	
	both ( $u, d, s, c, b$ )	–	$\mu^\pm N \rightarrow e^\pm N$	1 GeV	$\mathcal{O}_{\ell q}^{(1)}, \mathcal{O}_{\ell q}^{(3)}, \mathcal{O}_{qe}, \mathcal{O}_{eu}, \mathcal{O}_{lu}, \mathcal{O}_{ed}, \mathcal{O}_{ld}, \mathcal{O}_{ledq}, \mathcal{O}_{lequ}^{(1)}, \mathcal{O}_{lequ}^{(3)}$		
		$\mathcal{P}$	$\pi^0 \rightarrow \mu^\pm e^\mp$	150 GeV			
$\eta \rightarrow \mu^\pm e^\mp$			550 MeV				
$\eta' \rightarrow \mu^\pm e^\mp$			1 GeV				
$\tau^\pm \rightarrow \pi^0 \ell^\pm$			2 GeV				
$\mathcal{V}$		$\tau^\pm \rightarrow \rho^0 \ell^\pm$	2 GeV	$\mathcal{O}_{\ell q}^{(1)}, \mathcal{O}_{\ell q}^{(3)}, \mathcal{O}_{qe}, \mathcal{O}_{eu}, \mathcal{O}_{lu}, \mathcal{O}_{ed}, \mathcal{O}_{ld}, \mathcal{O}_{lequ}^{(3)}$			

TABLE IV: List of different LFV processes which are accessible to various experiments and corresponding  $2q2\ell$  operators that are significant for them at the tree-level. We have refrained from mentioning any other possible SMEFT operators beyond  $2q2\ell$  ones.

and  $K$  mesons. The other class of mesons include *heavy* quarks, bottom ( $B$  meson) and charm ( $D$  meson). All of these mesons can potentially give rise to LFV decays in both leptonic and semileptonic modes. Here we first discuss the latter type of decays, which can further be classified into two categories. First one is  $\mathcal{P} \rightarrow \mathcal{P}' \ell_i^- \ell_j^+$ , where the decay product of a pseudoscalar meson ( $\mathcal{P}$ ) contains another pseudoscalar meson  $\mathcal{P}'$  ( $\pi^0, \pi^\pm, K^0, K^\pm$  etc.). Fig. 1 represents a generic Feynman diagram corresponding to these processes. The quark composition of mesons considered for this analysis is given in Table-V.

#### 1. Pseudoscalar meson to pseudoscalar meson decays ( $\mathcal{P} \rightarrow \mathcal{P}' \ell_i^- \ell_j^+$ )

Exact expression of the branching ratio formula for semi-leptonic decays of pseudoscalar mesons can be quite involved (see e.g. Ref [24] for  $B$ -meson decays). Therefore, for simplicity we prefer to express the generic BR formula in terms of the effective coefficients ( $a_i$ ) associated with the



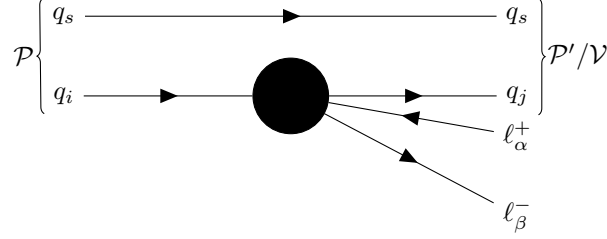


FIG. 1: Effective vertex for a LFV semi-leptonic decay of a pseudoscalar meson  $\mathcal{P}$  to a pseudoscalar  $\mathcal{P}'$  or a vector meson  $\mathcal{V}$ . The (anti-)quark  $q_i$  converts into another (anti-)quark  $q_j$  and two different flavors of leptons  $\ell_\alpha, \ell_\beta$ . The other (anti-)quark  $q_s$  represents the spectator (anti-)quark.

Pseudoscalars ( $\mathcal{P}$ )	Heavy Quark ( $c, b$ )	$B^0$	$B^+$	$B_s^0$	$D^0$	$D^+$	$D_s^+$
		$d\bar{b}$	$u\bar{b}$	$s\bar{b}$	$c\bar{u}$	$c\bar{d}$	$c\bar{s}$
	Light Quarks ( $u, d, s$ )	$K^+$	$K_{S(L)}^0$	$\pi^0$	$\pi^+$	$\eta$	$\eta'$
		$u\bar{s}$	$\frac{d\bar{s} \mp s\bar{d}}{\sqrt{2}}$	$\frac{u\bar{u} - d\bar{d}}{\sqrt{2}}$	$u\bar{d}$	$\frac{u\bar{u} + d\bar{d} - 2s\bar{s}}{\sqrt{6}}$	$\frac{u\bar{u} + d\bar{d} + s\bar{s}}{\sqrt{3}}$
Vectors ( $\mathcal{V}$ )		$\rho^0$	$\Upsilon$	$\omega$	$\phi$	$J/\psi$	
		$\frac{u\bar{u} - d\bar{d}}{\sqrt{2}}$	$b\bar{b}$	$\frac{u\bar{u} + d\bar{d}}{\sqrt{2}}$	$s\bar{s}$	$c\bar{c}$	

TABLE V: All mesons and their quark compositions under consideration in this analysis. They take part in LFV processes following Fig. 1 or Fig. 2.

relevant WCs (Eq.(6)) or their combinations, as:

$$\begin{aligned}
 \text{BR}(\mathcal{P} \rightarrow \mathcal{P}' \ell_i^- \ell_j^+) &= a_{VV} |C_{VV}|^2 + a_{AV} |C_{AV}|^2 + a_{TT} (|C_T|^2 + |C_{T_5}|^2) \\
 &+ a_{SS} |C_{SS}|^2 + a_{PS} |C_{PS}|^2 + a_{VS} \text{Re}[C_{VV} C_{SS}^*] \\
 &+ a_{AP} \text{Re}[C_{AV} C_{PS}^*] + a_{VT} \text{Re}[C_{VV} C_T^*] + a_{AT_5} \text{Re}[C_{AV} C_{T_5}^*]. \quad (7)
 \end{aligned}$$

• **LFV Decays of  $B$  meson:** LFVBDs are one of the most extensively studied processes in the search for NP. These decays have both leptonic and semileptonic modes. The semileptonic processes involve a bottom ( $b$ ) quark to strange ( $s$ ) quark transition along with two leptons ( $\ell_{i,j}, i \neq j$ ),  $b \rightarrow s \ell_i \ell_j$ . In literature they are found to be most popularly studied in terms of operators  $\mathcal{O}_9, \mathcal{O}_{10}, \mathcal{O}_S, \mathcal{O}_P, \mathcal{O}_T$  and their chiral counterparts [22, 89] and the branching fraction can be effectively expressed by Eq.(7).

• **LFV Decays of  $D$  meson:** Similarly, rare LFV  $D$  meson decays can happen in several modes *e.g.*,  $D^0 \rightarrow X^0 e^\pm \mu^\mp$  where  $X^0 = \pi^0, K_S^0, \bar{K}^{*0}, \rho^0, \phi, \omega, \eta$  [57] or  $D^+ \rightarrow \pi^+ e^\pm \mu^\mp$  *etc.*. Such processes are induced by  $c \rightarrow u \ell^+ \ell^-$ ,  $\ell = e, \mu$  where the  $|\Delta C| = 1$  effective weak Lagrangian can be written with two-step matching at the  $m_W$  scale and the  $m_c$  scale. Application of the EFT framework to these decays [71, 90, 91] also reveals that the differential decay rate in terms of the Wilson coefficients takes the general form of Eq.(7). It is to be noted here that, except  $\pi^0$  and  $K$  decay mode, other LFV decay modes couldn't be implemented in Flavio due to the unavailability of corresponding form factors.

• **LFV Decays of  $K$  meson:** In the presence of strong interaction and neglecting the top quark mass, the  $|\Delta S| = 1$  interactions responsible for the rare semi-leptonic  $K$  decays under

consideration are dominated by the four-quark operators  $\mathcal{O}_{1-6}$  as well as Gilman–Wise operators  $\mathcal{O}_{7X}$  ( $X = V, A$ ), with Wilson coefficients  $C_{7X}$  [92–94]. The decay rate for semileptonic processes like  $K^+ \rightarrow \pi^+ \ell_1^+ \ell_2^-$  and others take the form of Eq.(7). Due to composition of  $K_{L(S)}$  meson ( $= \frac{1}{\sqrt{2}}(\bar{s}d \pm \bar{d}s)$ ), one need to make the replacement for  $K_{L(S)} \rightarrow \pi^0$  decays as [78]:

$$C_{XY} \rightarrow \frac{(C_{XY})_{\alpha\beta 12} \mp (C_{XY})_{\alpha\beta 21}}{2} \quad C_{AB} \rightarrow \frac{(C_{AB})_{\alpha\beta 12} \pm (C_{AB})_{\alpha\beta 21}}{2} \quad (8)$$

where  $X, Y \in \{V, A\}$  and  $A, B \in \{S, P\}$ . The upper sign is for  $K_L$  while the lower is for  $K_S$ .

## 2. Pseudoscalar meson to vector meson decays ( $\mathcal{P} \rightarrow \mathcal{V} \ell_i^- \ell_j^+$ )

Similarly to pseudoscalar-to-pseudoscalar transition,  $\mathcal{P} \rightarrow \mathcal{V}$  transitions are also described by seven independent form factors which are usually determined by the light-cone QCD sum rule method [95–97] and can ultimately be expressed as,

$$\begin{aligned} \text{BR}(\mathcal{P} \rightarrow \mathcal{V} \ell_i^- \ell_j^+) &= a_{VV} |C_{VV}|^2 + a_{VA} |C_{VA}|^2 + a_{AV} |C_{AV}|^2 + a_{AA} |C_{AA}|^2 \\ &+ a_{PP} |C_{PP}|^2 + a_{SP} |C_{SP}|^2 + a_{AP} \text{Re}[C_{VA} C_{SP}^*] + a_{AS} \text{Re}[C_{AA} C_{PP}^*] \\ &+ a_{TT} (|C_T|^2 + |C_{T_5}|^2) + a_{ST} \text{Re}[C_{SP} C_T^*] + a_{PT} \text{Re}[C_{PP} C_T^*] \\ &+ a_{ST_5} \text{Re}[C_{SP} C_{T_5}^*] + a_{PT_5} \text{Re}[C_{PP} C_{T_5}^*]. \end{aligned} \quad (9)$$

## B. LFV leptonic decays of Pseudoscalar Mesons ( $\mathcal{P} \rightarrow \ell_i^- \ell_j^+$ ).

The generic expression for a pseudoscalar meson  $\mathcal{P}$  decaying to leptons ( $\ell_i^- \ell_j^+$ ), represented by a generic Feynman diagram in Fig. 2, can be summarized as:

$$\begin{aligned} \text{BR}(\mathcal{P} \rightarrow \ell_i^- \ell_j^+) &= \frac{\tau_{\mathcal{P}}}{128\pi m_{\mathcal{P}}^3 v^4} \sqrt{\lambda(m_{\mathcal{P}}, m_i, m_j)} \\ &\times \left( (m_{\mathcal{P}}^2 - (m_i + m_j)^2) \cdot \left| \sum_k f_{\mathcal{P}}^k \left( C_{VA}^k(m_i - m_j) + C_{SP}^k \frac{m_{\mathcal{P}}^2}{m_{q_1^k} + m_{q_2^k}} \right) \right|^2 \right. \\ &\left. + (m_{\mathcal{P}}^2 - (m_i - m_j)^2) \cdot \left| \sum_k f_{\mathcal{P}}^k \left( C_{AA}^k(m_i + m_j) + C_{PP}^k \frac{m_{\mathcal{P}}^2}{m_{q_1^k} + m_{q_2^k}} \right) \right|^2 \right) \end{aligned} \quad (10)$$

where summation over  $k$  runs over different quark-antiquark pairs of the meson,<sup>2</sup>  $v$  is the vacuum expectation value (vev),  $\tau_{\mathcal{P}}$  and  $m_{\mathcal{P}}$  are the lifetime and mass of  $\mathcal{P}$  respectively.  $m_{i,j}$  and  $m_{q_1,q_2}$  are the masses of leptons and quarks respectively. The decay constant  $f_{\mathcal{P}}$ , defined in terms of hadronic matrix element, and Källén  $\lambda$  function are given as:

$$\langle 0 | \bar{q}_2^k \gamma_\mu \gamma_5 q_1^k | \mathcal{P}(p) \rangle = i p_\mu f_{\mathcal{P}}^k, \quad (11)$$

$$\langle 0 | \bar{q}_2^k \gamma_5 q_1^k | \mathcal{P}(p) \rangle = i f_{\mathcal{P}}^k \frac{m_{\mathcal{P}}^2}{m_{q_1^k} + m_{q_2^k}}, \quad (12)$$

$$\lambda(a, b, c) = (a^2 - (b - c)^2)(a^2 - (b + c)^2), \quad (13)$$

<sup>2</sup> The summation over  $k$  is only required for mesons that are linear combinations of quark-antiquark pairs, such as  $K_{L(S)}$ ,  $\pi^0$ ,  $\eta$ , etc. For the others,  $f_{\mathcal{P}}^2$  can be written in the prefactor.

The hadronic matrix elements with scalar and vector densities vanish identically due to parity conservation. Also, due to the absence of the Lorentz structure, the tensor matrix element also vanishes. Thus, only the operators with pseudoscalar or axial-vector quark FCNC contribute, as evident from Eq. 10

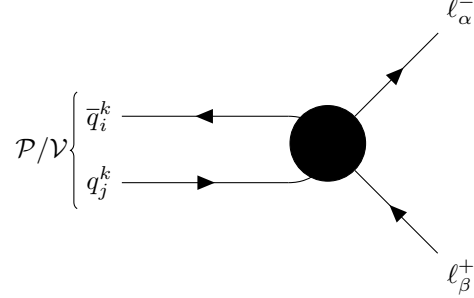


FIG. 2: Effective vertex of pseudoscalar/vector meson (or quarkonium) ( $\mathcal{P}/\mathcal{V}$ ) LFV decay to a pair of leptons via ( $2q2\ell$ ) operators.

### 1. LFV leptonic decays of light mesons ( $\pi^0, \eta, \eta'$ )

The effective Lagrangian ( $\mathcal{L}_{\text{eff}}$ ) for the decays of light-quark mesons ( $\pi^0, \eta, \eta'$ ) to two different flavors of leptons ( $\ell_i, \ell_j$ ), can be divided into a dimension-5 part,  $\mathcal{L}_{\text{dim-5}}$ ; a dimension-6 part,  $\mathcal{L}_{\text{dim-6}}$ ; and a dimension-7 gluonic part,  $\mathcal{L}_{\text{dim-7}}$  [29, 98, 99] depending upon the choice one might consider to include spin-dependent (SD) or independent contributions coming from the relevant operators. For our purpose we shall consider only  $2q2\ell$  type of operators as leading contributors, and the corresponding Lagrangian is given by Eq.(4). The resulting branching ratio for  $\mathcal{P}(\pi^0, \eta, \eta') \rightarrow \ell_i^- \ell_j^+$  is given by Eq.(10). However, the energy scale relevant for  $\pi^0$ -decays ( $\sim 100$  MeV) is too low to produce relevant results, and thus these decays are not included in this analysis.

### 2. LFV leptonic decays of $K$ , $D$ and $B$ mesons

In literature, EFT analysis of LFV Kaon decays is not plentiful and mainly found to be discussed in view of LFVBDs [71, 100, 101]. The decay rate for the process  $K_L \rightarrow \ell_i^+ \ell_j^-$  usually takes the form of Eq.(10). Discussion of leptonic LFVDDs in the EFT scenario can be found in [71, 102]. The branching fraction for such decays can also be translated to the above generic form. The most general form of branching fraction that can be found in literature for such LFV decays is usually given in terms of  $C_{9,10}$  etc [24].

## C. Leptonic LFV decays of Vector Quarkonia ( $\mathcal{V} \rightarrow \ell_i^- \ell_j^+$ )

In this section, we shall discuss the LFV decays of a subsection of vector mesons which have odd parity, same as pseudoscalar mesons, but total spin one. Vector mesons include rho ( $\rho$ ), phi ( $\phi$ ), omega ( $\omega$ ),  $J/\psi$   $\Upsilon$  mesons etc. Out of these,  $J/\psi$  and  $\Upsilon$  are collectively known as *quarkonia* ( $\mathcal{V}$ ) as they consist of a heavy quark and its antiquark. Their decays are known as LFV Quarkonium decays (LFVQDs) and in the following, we shall limit our analysis to these decays, as their theoretical and experimental results are more robust.

The general expression of branching fraction for such processes can be written as [29, 98, 103]

$$\begin{aligned} \text{BR}(\mathcal{V} \rightarrow \ell_i^- \ell_j^+) &= \frac{\tau_{\mathcal{V}} m_{\mathcal{V}}^3}{192\pi v^4} \left(1 - \frac{m_{\ell_j}^2}{m_{\mathcal{V}}^2}\right)^2 \\ &\times \left[ (f_{\mathcal{V}})^2 (|C_{VV}|^2 + |C_{AV}|^2) \left(1 + \frac{m_{\ell_j}^2}{2m_{\mathcal{V}}^2}\right) + 8 (f_{\mathcal{V}}^T)^2 (|\overline{C}_T|^2 + |\overline{C}_{T5}|^2) \left(1 + \frac{2m_{\ell_j}^2}{m_{\mathcal{V}}^2}\right) \right. \\ &\quad \left. + 12 f_{\mathcal{V}} f_{\mathcal{V}}^T \frac{m_{\ell_j}}{m_{\mathcal{V}}} \text{Re} (\overline{C}_T C_{VV}^* - \overline{C}_{T5} C_{AV}^*) \right], \quad \text{for } j > i. \end{aligned} \quad (14)$$

For  $j < i$ , one can replace  $m_{\ell_j} \rightarrow -m_{\ell_i}$ . The mass of the lighter lepton can be neglected. The decay constants  $f_{\mathcal{V}}$  and  $f_{\mathcal{V}}^T$  are defined as:

$$\langle 0 | \bar{q} \gamma^\mu q | \mathcal{V}(p, \epsilon) \rangle = m_{\mathcal{V}} \epsilon^\mu f_{\mathcal{V}}, \quad \langle 0 | \bar{q} \sigma^{\mu\nu} q | \mathcal{V}(p, \epsilon) \rangle = i f_{\mathcal{V}}^T (\epsilon^\mu p^\nu - \epsilon^\nu p^\mu). \quad (15)$$

Other hadronic matrix elements vanish again due to parity conservation, resulting in contributions only coming from the operators with vector and tensor quark FCNC. The WCs  $\overline{C}_{T(5)}$  are modified due to the leptonic dipole contributions as follows:

$$\begin{aligned} (\overline{C}_T)_{\alpha\beta ij} &= (C_T)_{\alpha\beta ij} - (eQ_i) \frac{m_\tau f_{\mathcal{V}}}{m_{\mathcal{V}} f_{\mathcal{V}}^T} (C_D)_{\alpha\beta} \delta_{ij} \\ (\overline{C}_{T5})_{\alpha\beta ij} &= (C_{T5})_{\alpha\beta ij} - (eQ_i) \frac{m_\tau f_{\mathcal{V}}}{m_{\mathcal{V}} f_{\mathcal{V}}^T} (C_{D5})_{\alpha\beta} \delta_{ij}. \end{aligned} \quad (16)$$

#### D. LFV $\tau$ decays

The Feynman diagram of LFV  $\tau$ -decays through  $2q2\ell$  effective vertex is given in Fig. 3. The quarks in the final states hadronise to form a meson. These LFV decays can also be further classified into two categories based on whether the final state meson is pseudoscalar ( $\tau \rightarrow \mathcal{P}\ell$ ) or vector ( $\tau \rightarrow \mathcal{V}\ell$ ).

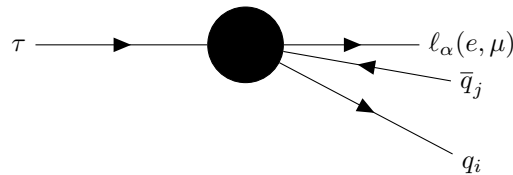


FIG. 3: Feynman diagram of LFV hadronic  $\tau$  decays. The blob indicates the charged LFV vertex.

### 1. Semileptonic $\tau$ decays ( $\tau \rightarrow \mathcal{V}\ell$ )

The generic expression for the branching ratio of  $\tau$  decays to vector meson and a lighter lepton  $\ell$  ( $e/\mu$ ) can be expressed as (neglecting  $m_\ell$ ) [78]:

$$\begin{aligned} \text{BR}(\tau^\pm \rightarrow \ell^\pm \mathcal{V}) &= \tau_\tau \frac{m_\tau^3}{256\pi v^4} \left(1 - \frac{m_\mathcal{V}^2}{m_\tau^2}\right)^2 \\ &\times \left[ (f_\mathcal{V})^2 \left(1 + \frac{2m_\mathcal{V}^2}{m_\tau^2}\right) (|C_{VV}|^2 + |C_{AV}|^2) + 32 (f_\mathcal{V}^T)^2 \left(1 + \frac{m_\mathcal{V}^2}{2m_\tau^2}\right) (|\overline{C}_T|^2 + |\overline{C}_{T_5}|^2) \right. \\ &\left. + 24 f_\mathcal{V}^T f_\mathcal{V} \frac{m_\mathcal{V}}{m_\tau} \text{Re} (\overline{C}_T C_{VV}^* - \overline{C}_{T_5} C_{AV}^*) \right] \end{aligned} \quad (17)$$

where  $m_\mathcal{V}$  and  $m_\tau$  are the vector meson and  $\tau$  mass respectively,  $\tau_\tau$  is the lifetime of the  $\tau$ . Other notations have a similar meaning to before. As the meson produced is a vector meson, the only non-vanishing hadronic matrix elements are of the vector and tensor type, same as the leptonic decay of a vector meson (sec-III C). As a result, only the vector and tensor WCs contribute. ( $\overline{C}_{T(5)}$ ) are also modified due to the presence of leptonic dipole WCs, as given in Eq.(16).

### 2. Semileptonic $\tau$ decays ( $\tau \rightarrow \mathcal{P}\ell$ )

Similar to the vector mesons, we take the expressions for the  $\tau$  decays to pseudoscalar mesons from Ref. [104]. The branching ratio for  $\tau \rightarrow \mathcal{P}\ell$ , with  $\ell = e, \mu$ , is given by (again, neglecting  $m_\ell$ )

$$\begin{aligned} \text{BR}(\tau \rightarrow \ell_i \mathcal{P}) &= \tau_\tau \frac{m_\tau^3}{256\pi v^4} \left(1 - \frac{m_\mathcal{P}^2}{m_\tau^2}\right)^2 \\ &\times \left[ \left| \sum_k f_\mathcal{P}^k \left( C_{VA}^k + \frac{m_\mathcal{P}^2 C_{SP}^k}{m_\tau(m_{q_1^k} + m_{q_2^k})} \right) \right|^2 + \left| \sum_k f_\mathcal{P}^k \left( C_{AA}^k - \frac{m_\mathcal{P}^2 C_{PP}^k}{m_\tau(m_{q_1^k} + m_{q_2^k})} \right) \right|^2 \right]. \end{aligned} \quad (18)$$

where  $k$  runs over flavour eigenstate quark-antiquark pairs of the meson. Similar to the case of leptonic decays of pseudoscalar mesons (sec-III B), the only surviving hadronic matrix elements are the pseudoscalar and axial-vector, resulting in contributions only from operators having quark FCNC with these Lorentz structures.

## E. Muon to electron conversion in nuclei ( $\text{CR}(\mu \rightarrow e, N)$ )

The LFV interaction Lagrangian for the  $\mu$ - $e$  transition in a nuclei is given by [105]:

$$\text{CR}(\mu \rightarrow e, N) = \frac{1}{\omega_{\text{capt}} v^4} \sum_{X \in \{L, R\}} \left| C_{e\gamma}^X D_N + \sum_{f \in \{p, n\}} \left( g_{XS}^f S_N^f + g_{XV}^f V_N^f \right) \right|^2 \quad (19)$$

where  $\omega_{\text{capt}}$  is the muon capture rate by the nucleus  $N$  and  $X$  runs over the chirality of the lepton FCNC. The dipole WCs can be obtained as  $C_{e\gamma}^R = C_{e\gamma}$  and  $(C_{e\gamma}^L)_{\alpha\beta} = (C_{e\gamma})_{\beta\alpha}^*$ . The fermion

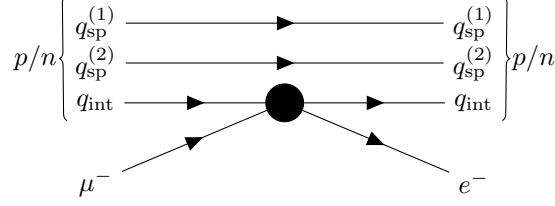


FIG. 4: Effective vertices of muon to electron conversion at a nucleus ( $N$ ).  $q \in \{u, d\}$  represents quarks with  $q_{\text{int}}$  and  $q_{\text{sp}}$  representing interacting and spectator quarks respectively. Apart from the interaction with the valence quarks shown in the figure, the muon can also interact with the sea quarks, resulting in scalar contributions from  $s$ -quarks as well [105].

flavour indices ( $\alpha\beta ij$ ) are suppressed. The effective couplings  $g$ 's are given in terms of LEFT WCs (Table-III) by,

$$g_{XS}^f = \sum_{q \in \{u, d, s\}} G_S^{q,f} (C_{eu(d)}^{S, XL} + C_{eu(d)}^{S, XR}) \quad (20)$$

$$g_{XV}^f = \sum_{q \in \{u, d\}} n_q^f (C_{eu(d)}^{V, XL} + C_{eu(d)}^{V, XR}) \quad (21)$$

with  $n_q^f$  being the number of valence  $q$ -quarks in  $f$  (neutron/proton). While summing over  $q$ , the coefficient  $C_{eu}(C_{ed})$  is used for  $u$ -type( $d$ -type) quarks. The coefficients  $G_S^{q,f}$  are defined in terms of matrix elements as,

$$\langle N | \bar{q}q | N \rangle = Z G_S^{q,p} \rho_p + (A - Z) G_S^{q,n} \rho_n \quad (22)$$

where  $Z, A$  are the atomic number and mass number of  $N$ , respectively,  $\rho_f$  denotes the density of the nucleon  $f$  within the nucleus. The matrix elements involving pseudo-scalar, axial-vector, and tensor quark currents vanish identically in this case. The numerical values of the relevant parameters, along with the values of the overlap integrals,  $D_N$ ,  $S_N$  and  $V_N$  [106], are provided in Table VI.

$N$	$\omega_{\text{capt}}$ [ $10^{-18}$ GeV]	$D_N$	$S$		$V$	
			$n$	$p$	$n$	$p$
Au	8.603	0.189	0.0918	0.0614	0.146	0.0974
Ti	1.705	0.0362	0.0435	0.0368	0.0468	0.0396

	$p$	$n$
$G_S^u$	5.1	4.3
$G_S^d$	4.3	5.1
$G_S^s$	2.5	2.5

TABLE VI: Numerical values of parameters relevant to  $\text{CR}(\mu \rightarrow e, N)$  used in Flavio.

#### IV. Calculation methods

As already mentioned, we use the Flavio package for computing the observables, which itself relies on the Wilson package for the running and matching of the SMEFT and LEFT WCs. Most of the observables considered in this work are already implemented in the Flavio package. However, several observables relevant to our analysis are not included in the default implementation. To address this, we extend the Flavio framework by incorporating these additional observables manually, using the generic expressions mentioned in sec-III. The parameters and other input data used for this purpose are provided in Tables-VII and VIII.

Decay Process	$a_{VV}$	$a_{AV}$	$a_{SS}$	$a_{PS}$	$a_{VS}$	$a_{AP}$	$a_{TT}$	$a_{VT}$	$a_{AT5}$
$D^+ \rightarrow \pi^+ e^- \mu^+$	0.0166	0.0166	0.0337	0.0337	-0.0066	0.0066	0.019	0.0081	0.0081
$D^0 \rightarrow \pi^0 e^- \mu^+$	0.00326	0.00326	0.0066	0.0066	-0.0013	0.0013	0.0038	0.0016	0.0016
$D_s^+ \rightarrow K^+ e^- \mu^+$	0.00622	0.00622	0.00893	0.00893	-0.002364	0.002364	0.00377	0.0025	0.0025
$K_L \rightarrow \pi^0 e^- \mu^+$	0.690	0.693	12.18	12.23	-3.19	3.24	-	-	-
$K^+ \rightarrow \pi^+ e^- \mu^+$	0.157	0.1578	2.71	2.72	-0.723	0.735	-	-	-

TABLE VII: Values of coefficients mentioned in Eq.(7) for various meson decay modes [78]. Entries marked with “-” indicate non-relevant data since tensor type WCs for down-type transitions are not contributing at dim-6. The coefficient for opposite lepton sign can be obtained by replacing  $a_{VS} \rightarrow -a_{VS}$ .

Meson	$\pi^0$	$K_L$	$K_S$	$D^0$	$\eta$	$\eta'$
<b>Lifetime [GeV<sup>-1</sup>]</b>	$1.28 \times 10^8$	$7.77 \times 10^{16}$	$1.36 \times 10^{14}$	$6.23 \times 10^{11}$	$7.63 \times 10^5$	$5.02 \times 10^3$

Decay constant	$f_{K_L}^{\bar{s}d} = f_{K_L}^{\bar{d}s}$	$f_{K_S}^{\bar{s}d} = -f_{K_S}^{\bar{d}s}$	$f_{\pi^0}^{\bar{u}u} = -f_{\pi^0}^{\bar{d}d}$	$f_{\eta}^{\bar{u}u} = f_{\eta}^{\bar{d}d}$	$f_{\eta}^{\bar{s}s}$	$f_{\eta'}^{\bar{u}u} = f_{\eta'}^{\bar{d}d}$	$f_{\eta'}^{\bar{s}s}$	$f_{D^0}^{\bar{u}c}$
<b>Value [MeV]</b>	109.9	109.9	130.2	100.3	-152.3	72.9	195.3	212.0

TABLE VIII: Lifetimes and decay constants used to implement the observables not included in Flavio.

To determine the bounds on the WCs in our analysis, we use a numerical minimiser. For each WC, the minimiser searches for the value for which the absolute difference between the prediction and the experimental limits is minimised ( $|\text{BR}_{\text{pred}} - \text{BR}_{\text{exp}}| \rightarrow 0$ ). This effectively identifies the largest value of the WC consistent with experimental data. Similarly, for the UV scale  $\Lambda$ , the minimiser finds the smallest possible value of  $\Lambda$  for which the predicted observable still satisfies the experimental constraint.

## V. Results and discussion

In order to obtain constraints on the LFV  $2q2\ell$  operators, we first identify the SMEFT operators ( $\mathcal{O}_{\alpha\beta ij}$ ), which are responsible for decays under consideration in this analysis, with exact flavour indices. Since we are considering charged lepton flavour-violating processes, it is necessary to have operators with lepton FCNC ( $\alpha \neq \beta$ ). However, the quark current in the operator can either be FCNC ( $i \neq j$ , *e.g.* for LFVBDs) or flavour conserving ( $i = j$ , *e.g.* for LFVQDs) as shown in Tables-IX and X respectively. Therefore, we plan to classify these two different kinds of coefficients separately and quote bounds on them coming from different experiments. Such classification also provides insight into specific operators that contribute dominantly to particular processes.

For the numerical analysis, we used the open source package Flavio [87]. For several decays, as mentioned in the caption of Table-I, we implemented the analytic expressions of the previous section into Python codes for the first time.



### A. 1-D Analysis

In the analysis of one-operator-at-a-time, we can extract two types of information which are complementary to each other. First, we can get constraints for different operators from different LFV processes. Second, assuming a perturbative SMEFT coefficient ( $|\mathcal{C}(\Lambda)| \leq 1$ ) we can probe the highest NP scale for each LFV observable. In the following, we discuss our results separately for  $\mu$  decay and  $\tau$  decay channels.

#### 1. $\mu - e$ sector

The availability of multiple LFV decay channels in the  $\mu - e$  sector provides a diverse set of complementary bounds on the Wilson coefficients considered in this analysis. This is evident from the fact that WCs can take a relatively weaker constraint  $\sim 10^2$  (*e.g.* see  $\eta$  LFV decay for  $[\mathcal{C}_{\ell q}^{(1)}]_{1212}$ ), as well as a very strong constraint  $\sim 10^{-6}$  for some others (*e.g.* see  $\text{CR}(\mu \rightarrow e)$  in Gold nuclei for  $[\mathcal{C}_{\ell q}^{(1)}]_{1211}$ ). Naturally, in the presence of a single operator at the high-energy scale, the constraints would be proportional to the precision of the experimental limit.

Along its vertical axis, Fig. 5 represents the limits on WCs of all vector LFV  $2q2\ell$  operators with indices given in both Tables-IX and X. In many cases, instead of a combined value, the experimental data for LFV decay channels with  $\ell_1^- \ell_2^+$  and  $\ell_1^+ \ell_2^-$  are reported separately. Therefore, we include both combinations in our analysis and present the corresponding results separately. If we look from bottom-up, for a particular observable, the figure gives us a complete picture of the relative strengths of all vector operators with different chirality. The horizontal axis shows the constraints on a particular WC coming from different processes.

Observables	Quark-level Process	Vector		Scalar	Tensor
		$\mathcal{O}_{\ell q}, \mathcal{O}_{\ell d}, \mathcal{O}_{ed}, \mathcal{O}_{\ell u}, \mathcal{O}_{eu}$	$\mathcal{O}_{qe}$	$\mathcal{O}_{\ell equ}^{(1)}, \mathcal{O}_{\ell edq}$	$\mathcal{O}_{\ell equ}^{(3)}$
$\text{BR}(K_L^0 \rightarrow e^\pm \mu^\mp)$	$\frac{d\bar{s}+s\bar{d}}{\sqrt{2}} \rightarrow e^\pm \mu^\mp$	$[\mathcal{O}]_{1212}, [\mathcal{O}]_{1221}$	$[\mathcal{O}]_{1212}, [\mathcal{O}]_{1221}$	$[\mathcal{O}]_{1212}, [\mathcal{O}]_{1221}, [\mathcal{O}]_{2112}, [\mathcal{O}]_{2121}$	-
$\text{BR}(K_L^0 \rightarrow \pi^0 e^\pm \mu^\mp)$	$\frac{d\bar{s}+s\bar{d}}{\sqrt{2}} \rightarrow d\bar{d}e^\pm \mu^\mp$	$[\mathcal{O}]_{1212}, [\mathcal{O}]_{1221}$	$[\mathcal{O}]_{1212}, [\mathcal{O}]_{1221}$	$[\mathcal{O}]_{1212}, [\mathcal{O}]_{1221}, [\mathcal{O}]_{2112}, [\mathcal{O}]_{2121}$	-
$\text{BR}(K^+ \rightarrow \pi^+ \mu^- e^+)$	$u\bar{s} \rightarrow u\bar{d}e^+ \mu^-$	$[\mathcal{O}]_{1212}$	$[\mathcal{O}]_{1212}$	$[\mathcal{O}]_{1212}, [\mathcal{O}]_{2121}$	-
$\text{BR}(K^+ \rightarrow \pi^+ \mu^+ e^-)$	$u\bar{s} \rightarrow u\bar{d}e^- \mu^+$	$[\mathcal{O}]_{1221}$	$[\mathcal{O}]_{1221}$	$[\mathcal{O}]_{1221}, [\mathcal{O}]_{2112}$	-
$\text{BR}(D^0 \rightarrow e^\pm \mu^\mp)$	$c\bar{u} \rightarrow e^\pm \mu^\mp$	$[\mathcal{O}]_{1212}, [\mathcal{O}]_{1221}$	$[\mathcal{O}]_{1212}, [\mathcal{O}]_{1221}$	$[\mathcal{O}]_{1212}, [\mathcal{O}]_{1221}, [\mathcal{O}]_{2112}, [\mathcal{O}]_{2121}$	$[\mathcal{O}]_{1212}, [\mathcal{O}]_{1221}, [\mathcal{O}]_{2112}, [\mathcal{O}]_{2121}$
$\text{BR}(D^+(D_s^+) \rightarrow \pi^+ e^+ \mu^-)$	$c\bar{d}(\bar{s}) \rightarrow u\bar{d}(\bar{s})e^+ \mu^-$	$[\mathcal{O}]_{1212}$	$[\mathcal{O}]_{1212}$	$[\mathcal{O}]_{1212}, [\mathcal{O}]_{2121}$	$[\mathcal{O}]_{1212}, [\mathcal{O}]_{2121}$
$\text{BR}(D^+(D_s^+) \rightarrow \pi^+ e^- \mu^+)$	$c\bar{d}(\bar{s}) \rightarrow u\bar{d}(\bar{s})e^- \mu^+$	$[\mathcal{O}]_{1221}$	$[\mathcal{O}]_{1221}$	$[\mathcal{O}]_{1221}, [\mathcal{O}]_{2112}$	$[\mathcal{O}]_{1221}, [\mathcal{O}]_{2112}$
$\text{BR}(B^{0(+)} \rightarrow K^{*0(+)} e^+ \mu^-)$	$d(u)\bar{b} \rightarrow d(u)\bar{s}e^+ \mu^-$	$[\mathcal{O}]_{1223}$	$[\mathcal{O}]_{2312}$	$[\mathcal{O}]_{1223}, [\mathcal{O}]_{2132}$	-
$\text{BR}(B^{0(+)} \rightarrow K^{*0(+)} e^- \mu^+)$	$d(u)\bar{b} \rightarrow d(u)\bar{s}e^- \mu^+$	$[\mathcal{O}]_{1232}$	$[\mathcal{O}]_{2321}$	$[\mathcal{O}]_{1232}, [\mathcal{O}]_{2123}$	-
$\text{BR}(B^{0(+)} \rightarrow \pi^{0(+)} e^\pm \mu^\mp)$	$d(u)\bar{b} \rightarrow d(u)\bar{d}e^\pm \mu^\mp$	$[\mathcal{O}]_{1213}, [\mathcal{O}]_{1231}$	$[\mathcal{O}]_{1312}, [\mathcal{O}]_{1321}$	$[\mathcal{O}]_{1213}, [\mathcal{O}]_{1231}, [\mathcal{O}]_{2113}, [\mathcal{O}]_{2131}$	-
$\text{BR}(B^0 \rightarrow \mu^\mp e^\pm)$	$\bar{d}\bar{b} \rightarrow \mu^\pm e^\mp$	$[\mathcal{O}]_{1213}, [\mathcal{O}]_{1231}$	$[\mathcal{O}]_{1312}, [\mathcal{O}]_{1321}$	$[\mathcal{O}]_{1213}, [\mathcal{O}]_{1231}, [\mathcal{O}]_{2113}, [\mathcal{O}]_{2131}$	-
$\text{BR}(B_s^0 \rightarrow \mu^\mp e^\pm)$	$\bar{s}\bar{b} \rightarrow \mu^\pm e^\mp$	$[\mathcal{O}]_{1223}, [\mathcal{O}]_{1232}$	$[\mathcal{O}]_{2312}, [\mathcal{O}]_{2321}$	$[\mathcal{O}]_{1223}, [\mathcal{O}]_{1232}, [\mathcal{O}]_{2123}, [\mathcal{O}]_{2132}$	-
$\text{BR}(B_s^0 \rightarrow \phi \mu^\pm e^\mp)$	$\bar{s}\bar{b} \rightarrow \bar{s}\bar{s}\mu^\pm e^\mp$	$[\mathcal{O}]_{1223}, [\mathcal{O}]_{1232}$	$[\mathcal{O}]_{2312}, [\mathcal{O}]_{2321}$	$[\mathcal{O}]_{1223}, [\mathcal{O}]_{1232}, [\mathcal{O}]_{2123}, [\mathcal{O}]_{2132}$	-

TABLE IX: Operators with different lepton and quark indices that have been analysed in this article. The second column represents the quark and lepton composition of the process. All vector operators under consideration have the same order of lepton and quark indices except  $\mathcal{O}_{qe}$ . Columns 5 and 6 show scalar and tensor operators, respectively.

All observables under consideration are arranged according to their decreasing order of experimental limits, starting from  $\text{CR}(\mu \rightarrow e) (\sim 10^{-13})$ , followed by  $K_L^0 \rightarrow e^\pm \mu^\mp (\sim 10^{-12})$  and so on. As explained in the caption of Fig. 5, the numbers shown represent the exponent  $x$  in the relation  $\mathcal{C}_{\text{max}} = 10^x$ , providing the maximum allowed value of the WC that satisfies the current experimental limit. The most stringent constraint on a given WC corresponds to the smallest (most negative) value of  $x$ . The boxes are also colour coded, with lighter shades starting from yellow, representing weaker constraints, whereas the darker boxes refer to a stronger constraint, as shown in the legend

Observables	Quark-level Process	Vector		Scalar	Tensor
		$\mathcal{O}_{\ell q}, \mathcal{O}_{\ell d}, \mathcal{O}_{\ell e}, \mathcal{O}_{\ell u}, \mathcal{O}_{\ell e}$	$\mathcal{O}_{qe}$	$\mathcal{O}_{\ell e q}^{(1)}, \mathcal{O}_{\ell e d q}$	$\mathcal{O}_{\ell e q}^{(3)}$
CR( $\mu \rightarrow e, \text{Au}$ )	$\mu (u/d/s) \rightarrow e (u/d/s)$	$[\mathcal{O}]_{1211}$	$[\mathcal{O}]_{1112}$	$[\mathcal{O}]_{1211}, [\mathcal{O}]_{2111}$	$[\mathcal{O}]_{1211}, [\mathcal{O}]_{2111}$
BR( $J/\Psi \rightarrow e^\pm \mu^\mp$ )	$c\bar{c} \rightarrow e^\pm \mu^\mp$	$[\mathcal{O}]_{1222}$	$[\mathcal{O}]_{2212}$	-	$[\mathcal{O}]_{1222}, [\mathcal{O}]_{2122}$
BR( $\Upsilon \rightarrow e^\mp \mu^\pm$ )	$b\bar{b} \rightarrow e^\pm \mu^\mp$	$[\mathcal{O}]_{1233}$	$[\mathcal{O}]_{3312}$	-	-
BR( $\pi^0 \rightarrow e^\pm \mu^\mp$ )	$\frac{u\bar{u}-d\bar{d}}{\sqrt{2}} \rightarrow e^\pm \mu^\mp$	$[\mathcal{O}]_{1211}$	$[\mathcal{O}]_{2111}$	$[\mathcal{O}]_{1211}, [\mathcal{O}]_{2111}$	$[\mathcal{O}]_{1211}, [\mathcal{O}]_{2111}$
BR( $\eta^0 \rightarrow e\mu$ )	$\frac{u\bar{u}+d\bar{d}-2s\bar{s}}{\sqrt{2}} \rightarrow e^\pm \mu^\mp$	$[\mathcal{O}]_{1211}, [\mathcal{O}]_{1222}$	$[\mathcal{O}]_{1112}, [\mathcal{O}]_{2212}$	$[\mathcal{O}]_{1211}, [\mathcal{O}]_{2111}, [\mathcal{O}]_{1222}, [\mathcal{O}]_{2122}$	$[\mathcal{O}]_{1211}, [\mathcal{O}]_{2111}, [\mathcal{O}]_{1222}, [\mathcal{O}]_{2122}$
BR( $\eta^{0'} \rightarrow e\mu$ )	$\frac{u\bar{u}+d\bar{d}+s\bar{s}}{\sqrt{2}} \rightarrow e^\pm \mu^\mp$	$[\mathcal{O}]_{1211}, [\mathcal{O}]_{1222}$	$[\mathcal{O}]_{1112}, [\mathcal{O}]_{2212}$	$[\mathcal{O}]_{1211}, [\mathcal{O}]_{2111}, [\mathcal{O}]_{1222}, [\mathcal{O}]_{2122}$	$[\mathcal{O}]_{1211}, [\mathcal{O}]_{2111}, [\mathcal{O}]_{1222}, [\mathcal{O}]_{2122}$

TABLE X: Operators with different lepton indices but same quark indices. Similar to Table-IX, the last three columns represent vector, scalar and tensor operators respectively.

of the figure. A missing entry corresponding to a particular WC-observable pair indicates that the operator is not relevant for that process and thus produces a very weak limit ( $\mathcal{C}_{\max} \geq (4\pi)^2$ ). In the following, we shall explain the limits in the figure systematically.

One can readily see that almost all the WCs of vector operators consisting of left-handed quark doublet current ( $\mathcal{C}_{\ell q}^{(1)}, \mathcal{C}_{\ell q}^{(3)}$  and  $\mathcal{C}_{qe}$ ) are constrained by most of the observables involving interaction of  $d$ -type quarks, despite the difference in the quark indices relevant to the process and that of the operator (see Tables-IX and X for details). Here we note that according to our convention, the running mass matrix of  $u_L$ -type quarks is diagonal at  $\Lambda$  (*Warsaw up* basis in *Wilson*), due to which WCs of operators with  $d_L$ -type quarks involve the CKM rotation as,

$$v^2 \mathcal{L}_{\text{LEFT}} \supset (\mathcal{C}_{ed}^{\text{fl}})_{\alpha\beta ij} (\mathcal{O}_{ed}^{\text{fl}})_{\alpha\beta ij} \equiv (\mathcal{C}_{ed}^{\text{fl}})_{\alpha\beta ij} (\bar{e}_\alpha \Gamma e_\beta) \left( \bar{d}_i^{\text{fl}} \Gamma d_j^{\text{fl}} \right) \quad (23)$$

$$\begin{aligned} &= (\mathcal{C}_{ed}^{\text{fl}})_{\alpha\beta ij} (\bar{e}_\alpha \Gamma e_\beta) \left( (\bar{d}_k^{\text{m}} V_{ki}^*) \Gamma (V_{jl} d_l^{\text{m}}) \right) \\ &= \left[ V_{ki}^* (\mathcal{C}_{ed}^{\text{fl}})_{\alpha\beta ij} V_{jl} \right] (\bar{e}_\alpha \Gamma e_\beta) \left( \bar{d}_k^{\text{m}} \Gamma d_l^{\text{m}} \right) \\ \Rightarrow & (\mathcal{C}_{ed})_{\alpha\beta kl}^{\text{m}} = V_{ki}^* (\mathcal{C}_{ed}^{\text{fl}})_{\alpha\beta ij} V_{jl} . \end{aligned} \quad (24)$$

where  $\mathcal{C}^{\text{m}}, \mathcal{C}^{\text{fl}}$  represent the WC of the operator involving quarks in mass eigenstates ( $\mathcal{O}^{\text{m}}$ ) and flavour eigenstates ( $\mathcal{O}^{\text{fl}}$ ), respectively. The mass eigenstate WCs receive contributions from all the flavour eigenstates WCs with different quark flavour indices, weighted by the corresponding CKM elements. Thus, depending on these elements, the observable becomes sensitive to WCs with all the flavour indices. Consequently, a constraint on the respective WC can be derived. On the other hand, observables with  $u$  and  $c$  quarks, namely decays of  $J/\psi$  and  $D$ -mesons requiring  $u_L$ -type LEFT operators, thus do not involve CKM. These observables provide reasonable constraints only on the relevant WCs mentioned in Tables-IX and X. Similarly, WCs of the operators with right-handed quark current ( $\mathcal{C}_{\ell d}, \mathcal{C}_{\ell e}, \mathcal{C}_{\ell u}$  and  $\mathcal{C}_{eu}$ ), also do not undergo the CKM rotation and are thus not constrained or weakly constrained by the observables with a different quark FCNC.

Another feature of the figure is that the processes considered with a combined limit on  $e^\pm \mu^\mp$  channels (e.g.,  $B^0 \rightarrow \pi^0 e^\pm \mu^\mp$ ) provide limits on WCs with both flavour index combinations  $\alpha\beta ij$  and  $\alpha\beta ji$  while the ones with separate limits constrain each index combination independently. This is because the operator with indices  $(\beta\alpha ij)$ , where lepton FCNC flow is opposite, is related to the one with indices  $(\alpha\beta ji)$  by a hermitian conjugation,

$$(\mathcal{C}_{\alpha\beta ji} (\bar{e}_\alpha \Gamma e_\beta) (\bar{q}_j \Gamma q_i))^\dagger = \mathcal{C}_{\alpha\beta ji}^* (\bar{e}_\beta \Gamma e_\alpha) (\bar{q}_i \Gamma q_j) . \quad (25)$$

Both of these operators appear in the Lagrangian to keep it real. Thus, while one of the indices combinations  $(\alpha\beta ij)$  and  $(\alpha\beta ji)$  is relevant to the process with  $e_\alpha^+ e_\beta^-$ , the other contributes to  $e_\alpha^- e_\beta^+$ . Hence, a combined experimental limit constrains both WCs simultaneously. Although decays of



FIG. 5: Upper bounds on the  $2q2\ell$  Wilson coefficient ( $\mathcal{C}_{\text{max}}$ ) involving first- and second-generation charged leptons ( $e^\pm$ ,  $\mu^\pm$ ), considering one at a time at scale  $\Lambda = 1 \text{ TeV}$ . Each box shows the constraint from a specific observable, colour-coded accordingly. The numerical value of the limit is given as  $\mathcal{C}_{\text{max}} = 10^x$ , where  $x$  is the value displayed in the box. The blank spaces represents  $\mathcal{C}_{\text{max}} \geq (4\pi)^2$ .

the  $K_L^0$  meson are considered with combined limits, they would exhibit similar behaviour due to its quark composition ( $\sim d\bar{s} + s\bar{d}$ ) even if the limits were not combined.

The classification of operators with indices according to the fermion composition of the decay process, as presented in Tables-IX and X, is particularly useful for interpreting the numerical results shown in Fig. 5. For example, it is evident from Table-X that for the coefficient  $\mathcal{C}_{1211}$ , stringent constraints might come from CR( $\mu \rightarrow e$ ) experiment and indeed it provides a strong bound  $\sim 10^{-6}$ . From Eqs. 20-21 we find that for a single-operator analysis, all seven operators of

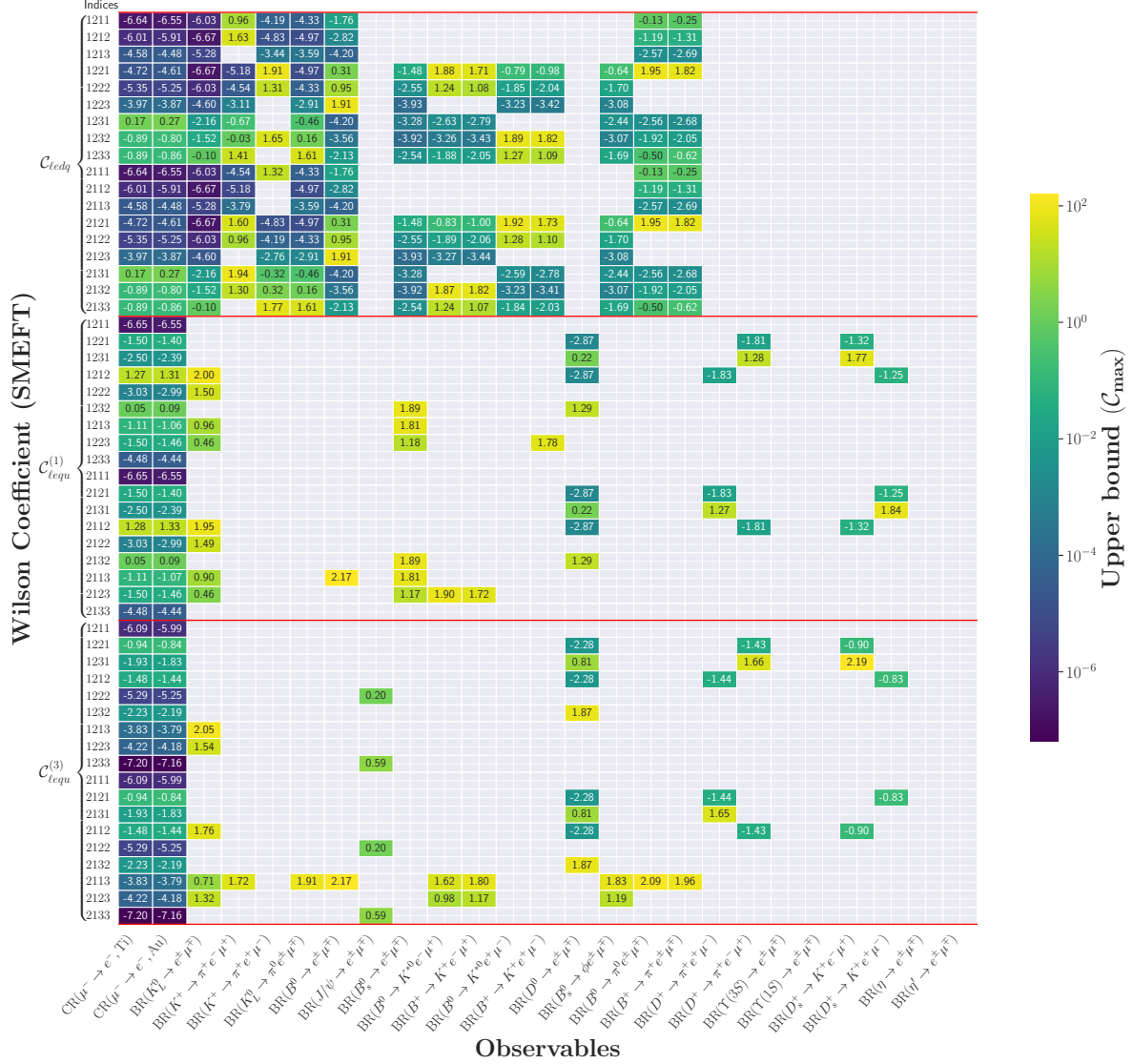


FIG. 6: Same as Fig. 5 but with scalar and tensor  $2q2\ell$  operators.

Fig. 5, with coefficients 1211, are contributing to the process with similar strength. This explains why all of them receive comparable constraints from this process. The WC  $(\mathcal{C}_{\ell q}^{(3)})_{1211}$ , however, is relatively less constrained. This is due to the opposite contributions of SMEFT operators to LEFT operators,  $(C_{eu}^{V,LL})_{1211}$  and  $(C_{ed}^{V,LL})_{1211}$ , during the matching (for details, see Appendix A). As a result, the proton and neutron contributions to the total amplitude interfere destructively. The other reason is that the experimental bounds on branching ratios of LFVKDs are almost as precise as  $\text{CR}(\mu \rightarrow e)$  followed by the LFVBDs. Turning our attention to the coefficients  $[\mathcal{O}]_{1222}$  and  $[\mathcal{O}]_{1233}$ , again, we see that they also receive strongest constraints,  $\sim 10^{-4}$  and  $\sim 10^{-3}$  respectively, from the  $\text{CR}(\mu \rightarrow e)$  experiment. Although  $C_{1222}$  is directly relevant to the decay of  $J/\psi$ , due to its small lifetime ( $\sim 10^{-20}$  sec), the branching ratio of this LFV decay gets suppressed and thus provides a very weak constraint. Also, as it involves  $u$ -type quark current, it does not constrain WCs with other indices. On the other hand, for  $\Upsilon$  LFV decay, in addition to its small lifetime ( $\sim 10^{-20}$  sec), a weak constraint is also caused by a weak experimental limit.

Similarly, from Table-IX we find that the coefficient  $\mathcal{C}_{1212}$  is most dominant for the LFVKDs

and LFVDDs, and therefore it should receive the most stringent constraints, specifically from these decays. Indeed comparing the numbers of Fig. 5 we find, for this coefficient and right-handed  $d$ -type quark current operators,  $\mathcal{C}_{\ell d}$  and  $\mathcal{C}_{ed}$ , LFVKDs provide the stringent constraint  $\sim 10^{-5}$ . On the other hand, for operators  $\mathcal{C}_{\ell q}^{(1)}, \mathcal{C}_{\ell q}^{(3)}$  and  $\mathcal{C}_{qe}$ , the strongest constraints with the upper limit  $\sim 10^{-6}$  come from  $\mu \rightarrow e$  conversion due to strong experimental limits and CKM enhancement of the relevant WC ( $C_{ed}^{V,LL}$ )<sub>1211</sub>, as explained earlier. For the coefficient  $\mathcal{O}_{1213}$  (1312 for  $\mathcal{C}_{qe}$ ), Table-IX indicates that a stringent limit should come from either  $B^0 \rightarrow e^\pm \mu^\mp$  or  $B^+(B^0) \rightarrow \pi^+(\pi^0)e^\pm \mu^\mp$  process. But the results of Fig. 5 show that the strongest limit of  $10^{-3}$  again derives from CR( $\mu \rightarrow e$ ), which can again be attributed to CKM contributions to ( $C_{ed}^{V,LL}$ )<sub>1211</sub>. This is also true for the operators  $\mathcal{C}_{\ell q}^{(1)}, \mathcal{C}_{\ell q}^{(3)}$  and  $\mathcal{C}_{qe}$ , all of which contain left-handed quark current. Also, as evident from Table-IX, the coefficient  $\mathcal{C}_{1223}$  ( $\mathcal{C}_{2312}$  for  $\mathcal{C}_{qe}$ ) and  $\mathcal{C}_{1232}$  ( $\mathcal{C}_{2321}$  for  $\mathcal{C}_{qe}$ ) are mostly responsible for processes involving  $s$ - $b$  quark FCNC and thus several LFVBD processes are expected to put strong constraints on these coefficients. Therefore, it explains why the most stringent constraints of  $\sim 10^{-3}$  for these WCs come from the processes  $B^0 \rightarrow K^{*0}e^-\mu^+$  and  $B^0 \rightarrow K^{*0}e^+\mu^-$  respectively.

Similar to Fig. 5, Fig. 6 represents the upper limits of scalar and tensor operators. Again Tables-IX and X guide us in understanding the results of this table. As before, CR( $\mu \rightarrow e$ ) proved to be the most sensitive process for the coefficient  $[\mathcal{O}]_{1211}$  of both scalar and tensor operators, with a limit  $\sim 10^{-6}$  GeV. Since most of the observables under consideration involve  $d$ -type quark current, the scalar operator  $\mathcal{C}_{ledq}$  receives significant constraints from several of those processes involving such current. Thus we find the process  $K_L^0 \rightarrow e^\pm \mu^\mp$  provides strongest constraints for several coefficients ( $[\mathcal{O}]_{1212}, [\mathcal{O}]_{1213}, [\mathcal{O}]_{1222}$ ) of  $\mathcal{C}_{ledq}$  operator. Likewise  $[\mathcal{O}]_{1231}, [\mathcal{O}]_{1232}$  and  $[\mathcal{O}]_{1233}$  receive strongest constraints from several LFVBD processes involving the  $b$  quark. To be specific,  $[\mathcal{C}_{ledq}]_{1231}$  is constrained by  $B^0 \rightarrow \mu^\mp e^\pm$  ( $\sim 10^{-4}$ ) whereas both  $[\mathcal{C}_{ledq}]_{1232}$  ( $\sim 10^{-4}$ ) and  $[\mathcal{C}_{ledq}]_{1233}$  ( $\sim 10^{-2}$ ) are constrained by  $B_s \rightarrow \mu^+ e^-$  process. These results are quite interesting considering the fact that for such LFVBDs, NP is expected to contribute via scalar or tensor operators. The contribution of tensor operators is usually quite negligible in these LFV processes, and thus they receive very weak constraints, as is evident from the results of this table.

An interesting observation from this Fig. 6 is the strong constraint ( $\sim 10^{-7}$ ) of 1233 (or 2133) coefficient for the tensor operator  $\mathcal{O}_{lequ}^{(3)}$  coming from CR( $\mu \rightarrow e$ ). From one-loop RGEs for Yukawa couplings of dimension-6 operators [82], we find that this is due to the effect of the photon dipole operator  $\mathcal{C}_{e\gamma}$  which provides a significant contribution to the CR( $\mu \rightarrow e$ ) transition.  $\mathcal{C}_{e\gamma}$  is related linearly to the leptonic dipole operators  $\mathcal{C}_{eW}$  and  $\mathcal{C}_{eB}$  ( $\mathcal{C}_{e\gamma} = \frac{1}{g_1}\mathcal{C}_{eB} - \frac{1}{g_2}\mathcal{C}_{eW}$ ) which are strongly dependent on this tensor operator in the following way,

$$\dot{\mathcal{C}}_{eW}^{rs} \sim -2g_2 C_{lequ}^{(3)} [Y_u]_{tp} + \dots, \quad \dot{\mathcal{C}}_{eB}^{rs} \sim 4g_1 C_{lequ}^{(3)} [Y_u]_{tp} + \dots, \quad (26)$$

where  $g_i$ 's are the gauge couplings and  $Y_u$  represents the Yukawa coupling of  $u$ -type quark. Similarly we also observe a limit ( $\sim 10^{-4}$ ) for the same coefficients but for the scalar operator  $\mathcal{O}_{lequ}^{(1)}$ . But the origin of this constraint can be traced to the Gauge RGEs [83] of these operators instead, where they are related to each other as well as with the dipole operator  $\mathcal{C}_{eW}$ , as can be seen from the equation below

$$\dot{\mathcal{C}}_{lequ}^{(3)} = \frac{3}{8}g_2^2 C_{lequ}^{(1)} + \left(N_c - \frac{1}{N_c}\right) g_3^2 C_{lequ}^{(3)} - \frac{3}{2}g_2 \mathcal{C}_{eW} [Y_u^\dagger]_{st} + \dots, \quad (27)$$

where  $N_c = 3$  is the number of colors.

Fig. 7 shows the maximum values of the new physics scale  $\Lambda$  accessible by each of these operators in the  $\mu$ - $e$  sector for single operator analysis. Different colour codes represent different energy values, from  $10^2$  GeV to  $10^6$  GeV, as shown in the legend, and the numbers in boxes give exact

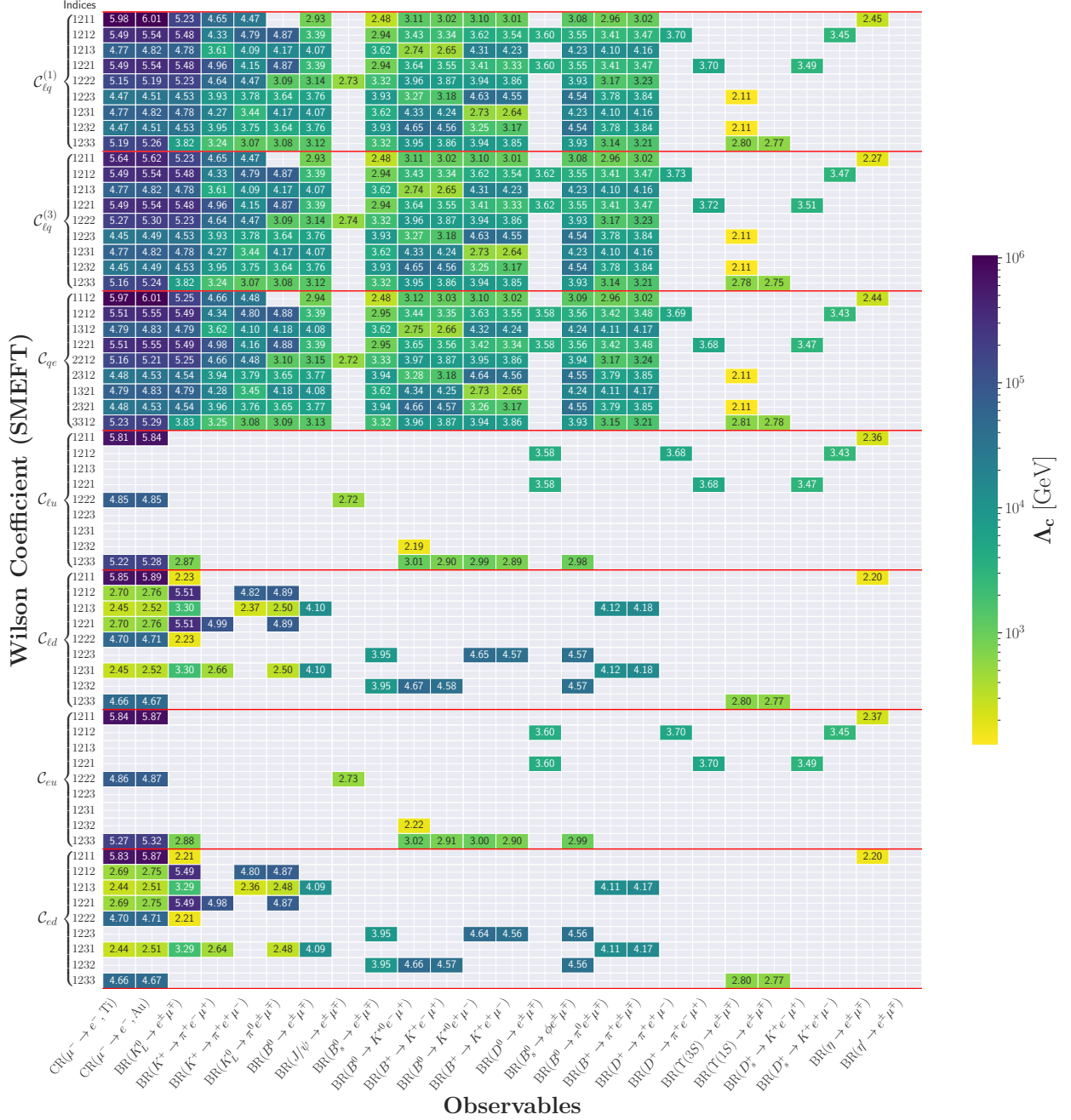


FIG. 7: Upper bounds on the UV scale for each  $2q2\ell$  Operator ( $\Lambda_c$ ) involving first- and second-generation charged leptons ( $e^\pm, \mu^\pm$ ), considering  $\mathcal{C} = 1$ . Each box shows the constraint from a specific observable, colour-coded accordingly. The numerical value of the limit is given as  $\Lambda_c = 10^x$ , where  $x$  is the value displayed in the box, thus representing a stringent constraint for larger numbers (darker box).

exponential values. To produce these numbers, we kept the value of the particular perturbative WC fixed to unity at 1 TeV and then varied  $\Lambda$  to satisfy the experimental limit of each observable (minimum entry-level value of this figure was kept fixed at 125 GeV). This being the reverse process of producing numbers of Fig. 5, we also find a similar trend exists among the numbers of these two figures. Clearly,  $CR(\mu \rightarrow e)$  is the most sensitive process for most of the diagonal



elements,  $([C]_{1211,1222,1233})$ , ranging from  $10^4 - 10^6$  GeV irrespective of the chirality. This is followed by the process  $K_L^0 \rightarrow e^\pm \mu^\mp$ , which is almost equally sensitive for the coefficients of  $\mathcal{C}_{\ell q}^{(1)}, \mathcal{C}_{\ell q}^{(3)}$  and  $\mathcal{C}_{qe}$ . Therefore, it can be concluded that for a single-operator dominance, 1211, 1212, 1213 and 1222 coefficients of left-handed quark current operators can be probed competitively by  $\text{CR}(\mu \rightarrow e)$  or  $K_L^0 \rightarrow e^\pm \mu^\mp$  process. For the right-handed quark current operators, situations are a little more distributed. For the coefficients 1211 and 1222,  $\text{CR}(\mu \rightarrow e)$  can probe the highest energy scale, whereas to probe 1212, the relevant experiment is  $K_L^0 \rightarrow e^\pm \mu^\mp$ .

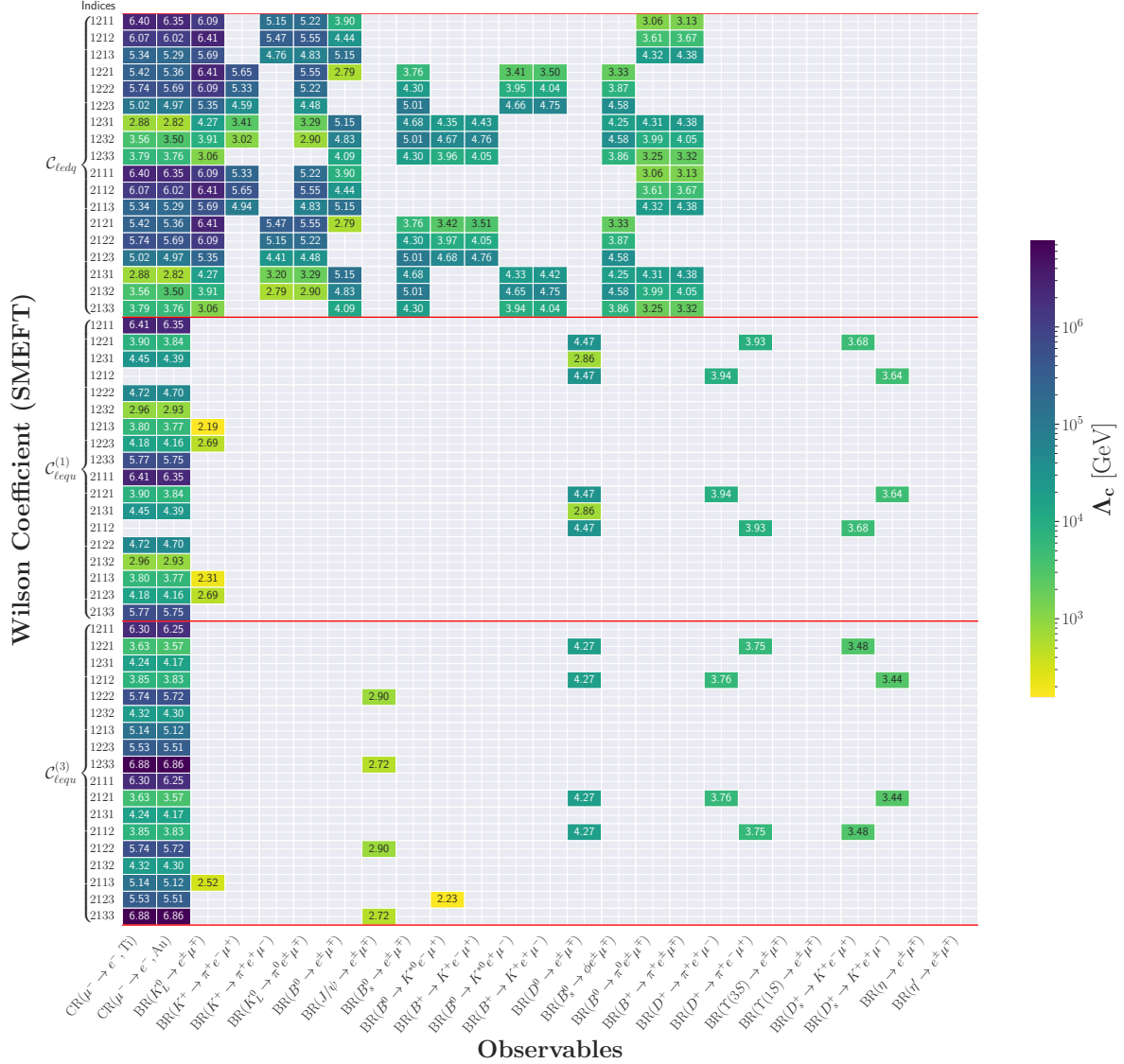


FIG. 8: Same as Fig. 7 but with scalar and tensor operators.

On the other hand, several LFVBD processes are most sensitive at  $\sim 10^3 - 10^5$  GeV for the coefficients 1213, 1223 (or 1312, 2312) for all left-handed and  $d$ -type right-handed quark current operators. Also, except  $[\mathcal{O}]_{1222}$  for  $J/\Psi$  or  $[\mathcal{O}]_{1233}$  for  $\Upsilon(1S)$ , LFVQDs are found to be least sensitive to other operators and coefficients. For LFVDD processes, they can probe the  $[C]_{1212}$  coefficients of right-handed  $u$ -type quark-current operators  $\sim 10^3$  GeV, but their chiral counterparts are dominated by  $\text{CR}(\mu \rightarrow e)$ . Therefore we can conclude that if any physics that might generate these operators with couplings  $(C/\Lambda^2)$  within the range  $1/(10^6 \text{ GeV})^2 - 1/(10^4 \text{ GeV})^2$ , it is expected



that  $\text{CR}(\mu \rightarrow e)$ ,  $K_L^0 \rightarrow e^\pm \mu^\mp$  or several LFVBDs can be observed in future experiments.

The maximum energy values that can be probed by these scalar and tensor operators are shown in Fig. 8. Looking at the range of  $\Lambda$  we can again conclude that for any new physics that might generate the scalar operator  $\mathcal{C}_{ledq}$  with couplings  $(\mathcal{C}/\Lambda^2)$  within the range  $1/(10^6 \text{ GeV})^2 - 1/(10^2 \text{ GeV})^2$ , it is expected that  $\text{CR}(\mu \rightarrow e)$ , all LFVKDs or several LFVBDs can be observed in future experiments. On the other hand, for the scalar operator  $\mathcal{C}_{lequ}^{(1)}$  or the tensor operator  $\mathcal{C}_{lequ}^{(3)}$  the same range of coupling is relevant for  $\text{CR}(\mu \rightarrow e)$ , LFVDDs and LFV decays of  $J/\psi$ .

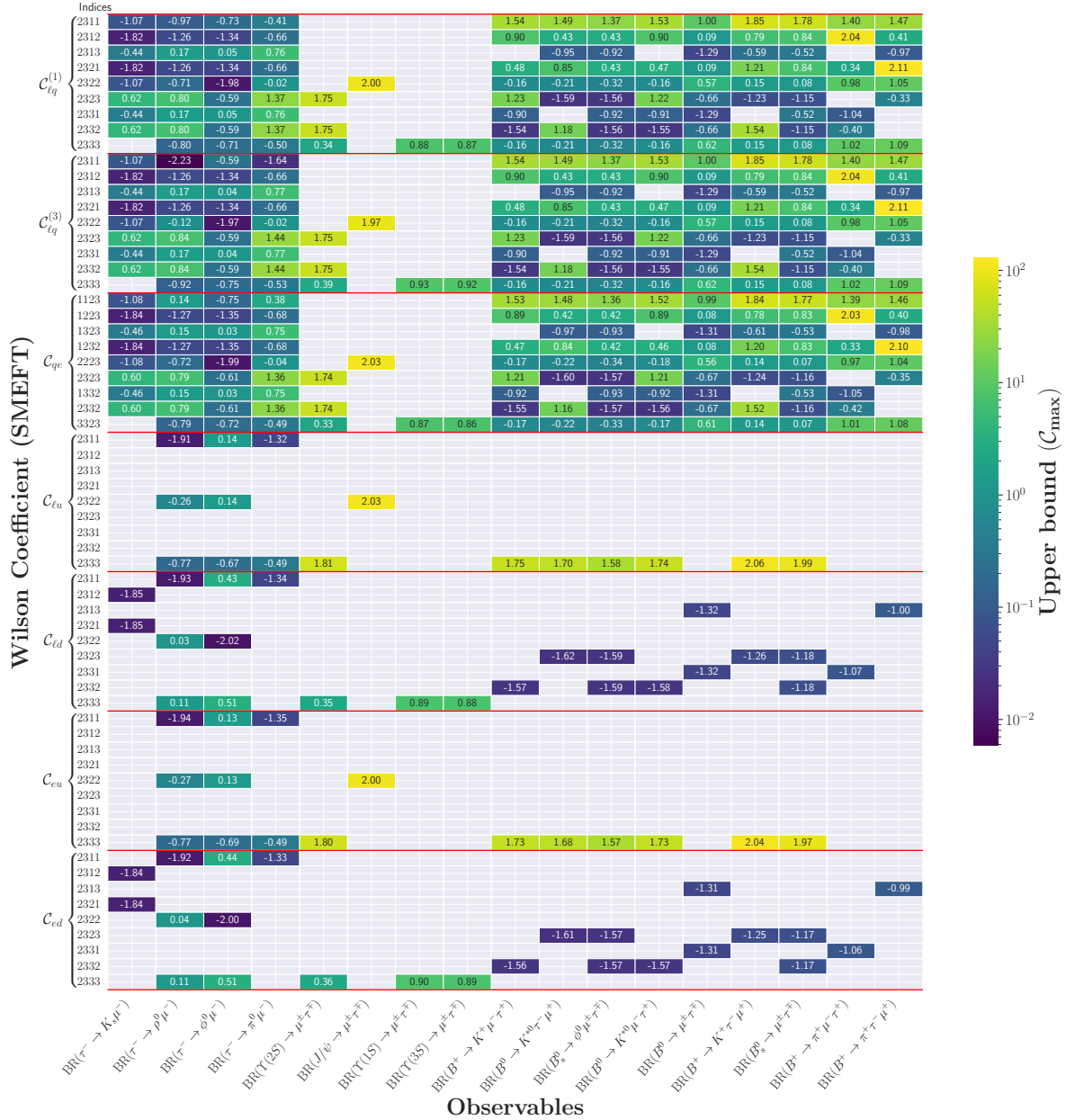


FIG. 9: Same as Fig. 5 but with observables and operators with second- and third-generation charged leptons ( $\mu^\pm, \tau^\pm$ ).

## 2. $\tau\text{-}\ell(e, \mu)$ sector

Similar to  $\mu\text{-}e$  sector, the  $\tau\text{-}\ell(e, \mu)$  sector results are shown in Figs. 9-14. A couple of significant differences from  $\mu\text{-}e$  sector are the following. First, the WCs in this sector are significantly less constrained. Compared to the 8 orders of magnitude spread of WCs in the  $\mu$  sector, WCs relevant for the  $\tau$  sector vary only 4 orders of magnitude, from  $10^{-2}$  to  $10^2$ . The reason for this is that the experimental values of LFV  $\tau$  decays are a few orders of magnitude less precise compared to those of  $\mu$  decays. The second difference is the presence of more empty boxes for operators with right-handed  $u$ -type quark current (in both  $e$  and  $\mu$  decays). This signifies less importance of these operators for  $\tau$  LFV decays. On the contrary, operators with right-handed  $d$ -type quark current ( $\mathcal{C}_{\ell d}, \mathcal{C}_{ed}$ ) are relatively significant because the LFV processes which are considered here mostly involve  $d$ -type quark transitions. In the following, we shall discuss the results of  $\tau \rightarrow \mu$  decays only. We observed a similar trend of results for  $\tau \rightarrow e$  decays, and they have been included in Appendix-B for completeness.

Observables	Quark-level Process	Vector		Scalar	Tensor
		$\mathcal{O}_{\ell q}, \mathcal{O}_{\ell d}, \mathcal{O}_{ed}, \mathcal{O}_{\ell u}, \mathcal{O}_{eu}$	$\mathcal{O}_{qe}$	$\mathcal{O}_{\ell equ}^{(1)}, \mathcal{O}_{\ell edq}$	$\mathcal{O}_{\ell equ}^{(3)}$
BR( $\tau^+ \rightarrow K_s^0 \mu^+$ )	$\tau^+ \rightarrow \frac{1}{\sqrt{2}} (d\bar{s} - \bar{d}s) \mu^+$	$[\mathcal{O}]_{2312}, [\mathcal{O}]_{2312}$	$[\mathcal{O}]_{1223}$	$[\mathcal{O}]_{2312}, [\mathcal{O}]_{2321}, [\mathcal{O}]_{3212}, [\mathcal{O}]_{3221}$	-
BR( $\tau^+ \rightarrow \pi^0 \mu^+$ )	$\tau^+ \rightarrow \frac{1}{\sqrt{2}} (u\bar{u} - d\bar{d}) \mu^+$	$[\mathcal{O}]_{2311}$	$[\mathcal{O}]_{1123}$	$[\mathcal{O}]_{2311}, [\mathcal{O}]_{3211}$	$[\mathcal{O}]_{2311}, [\mathcal{O}]_{3211}$
BR( $\tau^+ \rightarrow \rho^0 \mu^+$ )	$\tau^+ \rightarrow \frac{1}{\sqrt{2}} (u\bar{u} - d\bar{d}) \mu^+$	$[\mathcal{O}]_{2311}$	$[\mathcal{O}]_{1123}$	-	$[\mathcal{O}]_{2311}, [\mathcal{O}]_{3211}$
BR( $\tau^+ \rightarrow \phi^0 \mu^+$ )	$\tau^+ \rightarrow s\bar{s} \mu^+$	$[\mathcal{O}]_{2322}$	$[\mathcal{O}]_{2223}$	-	-
BR( $B^0 \rightarrow \tau^\pm \mu^\mp$ )	$d\bar{b} \rightarrow \tau^\pm \mu^\mp$	$[\mathcal{O}]_{2313}, [\mathcal{O}]_{2331}$	$[\mathcal{O}]_{1323}, [\mathcal{O}]_{1332}$	$[\mathcal{O}]_{2313}, [\mathcal{O}]_{2331}, [\mathcal{O}]_{3213}, [\mathcal{O}]_{3231}$	-
BR( $B^{0(+)} \rightarrow K^{*0(+)} \tau^+ \mu^-$ )	$d(u)\bar{b} \rightarrow d(u)\bar{s} \tau^+ \mu^-$	$[\mathcal{O}]_{2332}$	$[\mathcal{O}]_{2332}$	$[\mathcal{O}]_{2332}, [\mathcal{O}]_{3223}$	-
BR( $B^{0(+)} \rightarrow K^{*0(+)} \tau^- \mu^+$ )	$d(u)\bar{b} \rightarrow d(u)\bar{s} \tau^- \mu^+$	$[\mathcal{O}]_{2323}$	$[\mathcal{O}]_{2323}$	$[\mathcal{O}]_{2323}, [\mathcal{O}]_{3232}$	-
BR( $B^+ \rightarrow \pi^+ \tau^+ \mu^-$ )	$u\bar{b} \rightarrow u\bar{d} \tau^+ \mu^-$	$[\mathcal{O}]_{2331}$	$[\mathcal{O}]_{1332}$	$[\mathcal{O}]_{2331}, [\mathcal{O}]_{3213}$	-
BR( $B^+ \rightarrow \pi^+ \tau^- \mu^+$ )	$u\bar{b} \rightarrow u\bar{d} \tau^- \mu^+$	$[\mathcal{O}]_{2313}$	$[\mathcal{O}]_{1323}$	$[\mathcal{O}]_{2313}, [\mathcal{O}]_{3231}$	-
BR( $B_s^0 \rightarrow \tau^\pm \mu^\mp$ )	$s\bar{b} \rightarrow \tau^\pm \mu^\mp$	$[\mathcal{O}]_{2323}, [\mathcal{O}]_{2332}$	$[\mathcal{O}]_{2323}, [\mathcal{O}]_{2332}$	$[\mathcal{O}]_{2323}, [\mathcal{O}]_{2332}, [\mathcal{O}]_{3223}, [\mathcal{O}]_{3232}$	-
BR( $B_s^0 \rightarrow \phi^0 \tau^\pm \mu^\mp$ )	$s\bar{b} \rightarrow s\bar{s} \tau^\pm \mu^\mp$	$[\mathcal{O}]_{2323}, [\mathcal{O}]_{2332}$	$[\mathcal{O}]_{2323}, [\mathcal{O}]_{2332}$	$[\mathcal{O}]_{2323}, [\mathcal{O}]_{2332}, [\mathcal{O}]_{3223}, [\mathcal{O}]_{3232}$	-
BR( $J/\psi \rightarrow \tau^\pm \mu^\mp$ )	$c\bar{c} \rightarrow \tau^\pm \mu^\mp$	$[\mathcal{O}]_{2322}$	$[\mathcal{O}]_{2223}$	-	$[\mathcal{O}]_{2322}, [\mathcal{O}]_{3222}$
BR( $\Upsilon \rightarrow \tau^\pm \mu^\mp$ )	$b\bar{b} \rightarrow \tau^\pm \mu^\mp$	$[\mathcal{O}]_{2333}$	$[\mathcal{O}]_{3323}$	-	-

TABLE XI: Operators with indices for different LFV decay modes which include  $\tau$  and  $\mu$  leptons. The operators relevant for the processes where  $e$  is in the final states instead of  $\mu$  can be obtained by replacing the indices as  $\{ij23, ij32\} \rightarrow \{ij13, ij31\}$  for  $\mathcal{O}_{qe}$  and  $\{23ij, 32ij\} \rightarrow \{13ij, 31ij\}$  for other operators.

Following Table-XI we find that the coefficient  $\mathcal{C}_{2311}$  is relevant for a couple of pseudoscalar meson decays of  $\tau$  and thus the strongest constraint is expected from any of them. Indeed it is found from Fig. 9 that the process  $\tau^\pm \rightarrow \rho^0 \mu^\pm$  provides the strongest constraint, although weak ( $\sim 10^{-2}$ ), for the  $\mathcal{C}_{2311}$  (or  $\mathcal{C}_{1123}$ ) coefficient of all operators except  $\mathcal{C}_{\ell q}^{(1)}$  and  $\mathcal{C}_{qe}$ . For these two operators same order of constraints are obtained from  $\tau \rightarrow K_s \mu$  decay as  $\tau \rightarrow \pi^0 \mu$  involves contributions from both  $u$  and  $d$  operators, which interfere destructively due to equal and opposite contributions from these operators. The coefficient  $\mathcal{C}_{2322}$  is primarily responsible for  $\tau \rightarrow \phi \mu$  or  $J/\psi \rightarrow \tau^\pm \mu^\mp$  decays. The former one, being experimentally more precise, provides the strongest constraint ( $\sim 10^{-2}$ ) for this coefficient for all left-handed quark current operators. The same is true for the right-handed quark current with  $d$ -type transition as well.

Similarly, the coefficient  $\mathcal{C}_{2312}$  (or  $\mathcal{C}_{2321}$ ) is the dominant contributor to the decay  $\tau \rightarrow K_s \mu$ , as mentioned in Table-XI and thus receives the strongest constraint from this decay for all operators. All LFVBDs are responsible for  $\mathcal{C}_{2313, 2331}$  (or  $\mathcal{C}_{1332, 1323}$ ),  $\mathcal{C}_{2323, 2332}$  (or  $\mathcal{C}_{2323, 2332}$ ) and  $\mathcal{C}_{3223}$  coefficients as they involve  $b$  quark transitions. It was shown in Ref. [26] that for a single operator

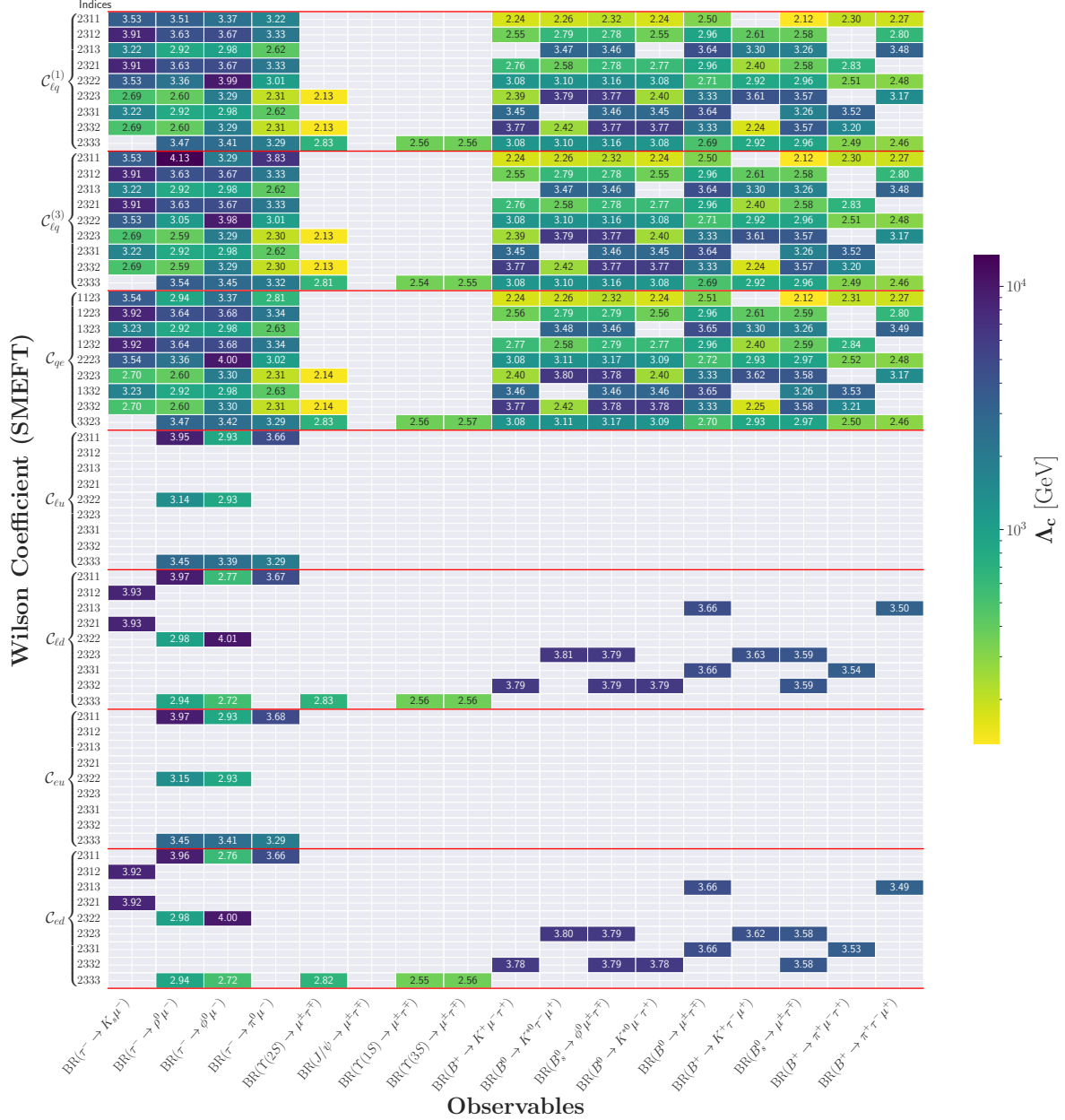


FIG. 10: Same as Fig. 7 but with observables and operators with second- and third-generation charged leptons ( $\mu^\pm, \tau^\pm$ ).

dominance in LFVBDs, these coefficients contribute most significantly for the operators  $\mathcal{C}_{\ell q}^{(1)}, \mathcal{C}_{\ell q}^{(3)}$ ,  $\mathcal{C}_{qe}$ ,  $\mathcal{C}_{ld}$  and  $\mathcal{C}_{ed}$ . We find our results, from Table-XI, to be consistent with the same as constraints of similar magnitude ( $\sim 10^{-2}$ ) on these coefficients come from different  $B$  decay processes. Being responsible for  $u$ -type quark transition only, operators  $\mathcal{C}_{lu}$  and  $\mathcal{C}_{eu}$  do not contribute to these LFVBDs.

We probe the maximum attainable energy scales obtained from  $\tau$ - $\mu$  sector LFV decays in Fig. 10. Clearly we find that most the off-diagonal coefficients ( $[\mathcal{C}]_{2313}$  etc.) of this sector are probed by different LFVBDs at  $10^3$  GeV, whereas the diagonal coefficients ( $[\mathcal{C}]_{2311}$  etc.) are probed by different LFV  $\tau$  decay experiments at slightly higher energies,  $\sim 10^4$  GeV.

Analysis of constraints on scalar and tensor operators and corresponding accessible energy ranges for  $\tau$ - $\mu$  sector are shown in Figs. 11 and 12 respectively. Since LFVBDs involve  $d$ -type quark transitions, it is obvious that the scalar operator  $\mathcal{C}_{\ell edq}$  plays a significant role in those decay processes and thus can be probed by these decays at  $10^3 - 10^4$  GeV.

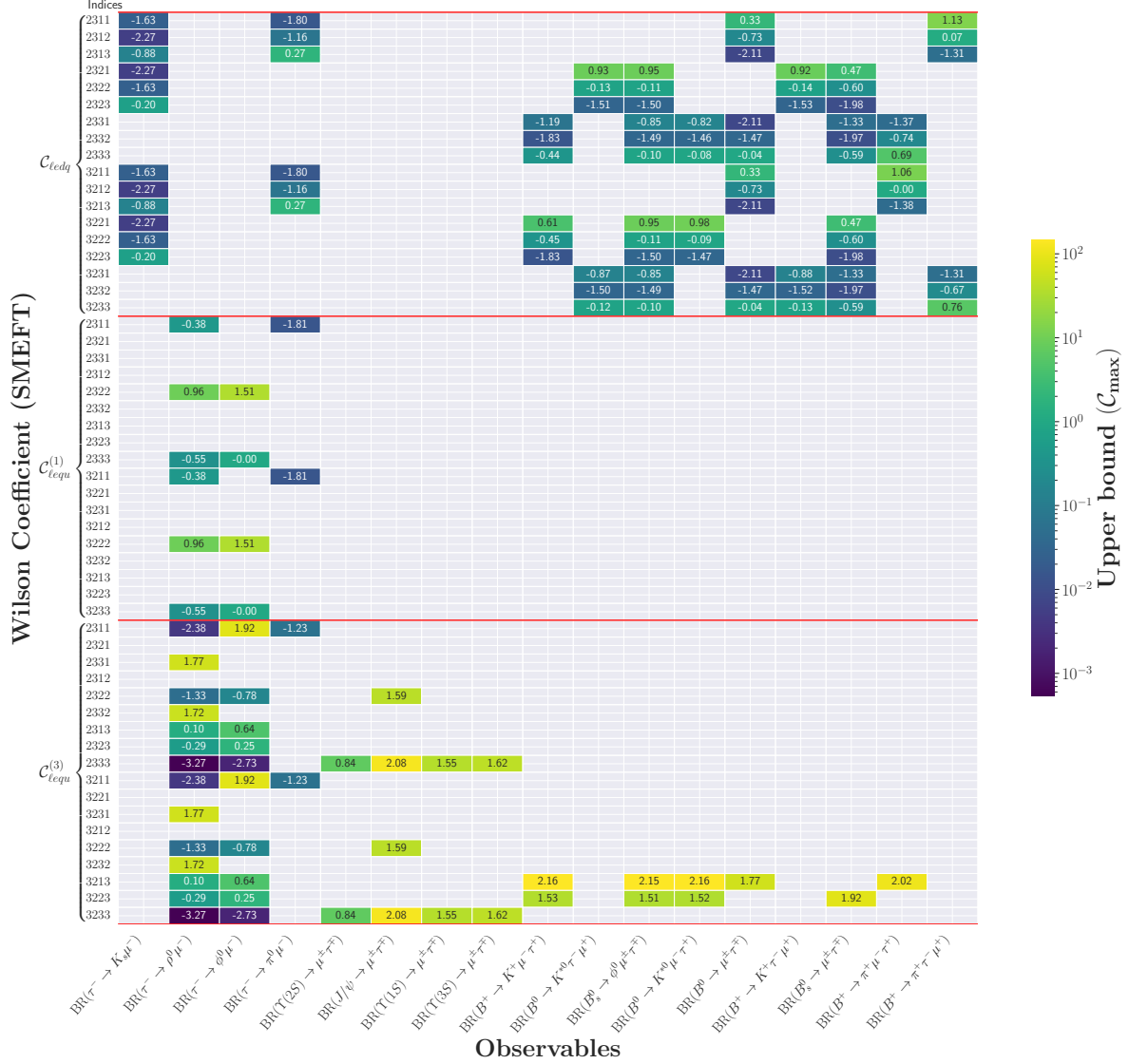


FIG. 11: Same as Fig. 9 but with scalar and tensor  $2q2\ell$  operators.

## VI. 2-D Analysis

It is quite reasonable to expect that several of these  $2q2\ell$  operators are generated at the high-energy scale  $\Lambda$ , unless compelled by some additional symmetry or other argument. Therefore, in this section, we represent our result for 2-D analysis or two-parameter fits, meaning that when two operators are simultaneously present at the new physics scale by some UV dynamics, while other operators are zero. These analyses can provide useful information on the interplay between the WCs of these operators due to the RGE running. They can also give some intuitive insight about

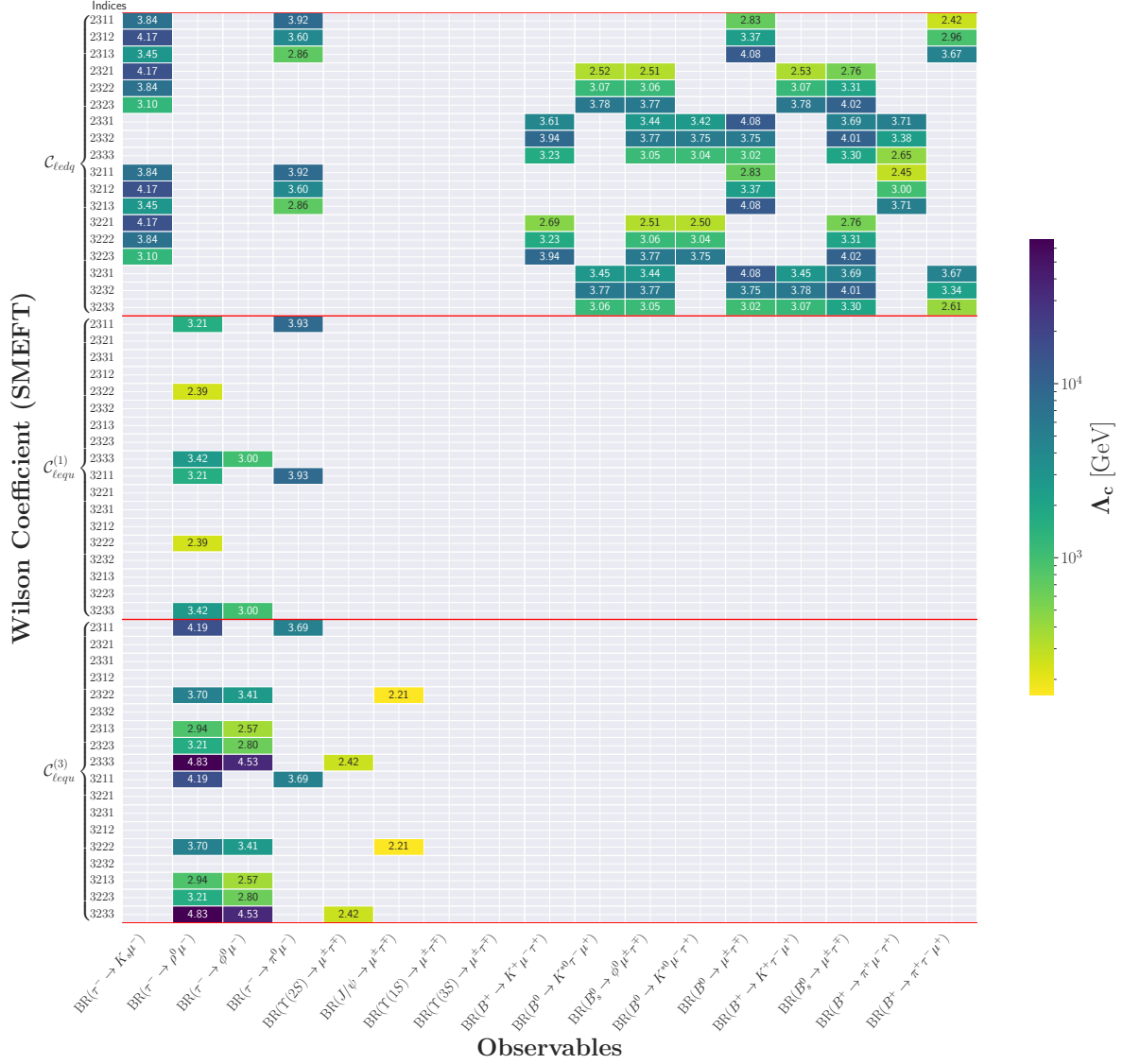


FIG. 12: Same as Fig. 10 but with scalar and tensor operators.

their correlation by highlighting the most constrained combinations among them. Out of several possible pairs, we show here a couple of them which are interesting.

In Fig. 13 we show the branching ratios of two most constrained LFV processes,  $\text{CR}(\mu \rightarrow e)$  (red) and  $K_L^0 \rightarrow e^\pm \mu^\mp$  (blue), as functions of the Wilson coefficients  $[\mathcal{C}_{\ell q}^{(3)}]_{1212}$  and  $[\mathcal{C}_{ed}]_{1212}$  on a logarithmic scale. We choose to show only the positive values of the right-handed quark current Wilson coefficient  $\mathcal{C}_{ed}$  against both positive and negative values of the left-handed quark current coefficient  $\mathcal{C}_{\ell q}^{(3)}$ . The dotted lines and colored regions represent the limits of the coefficients obtained from 1-D and 2-D analysis, respectively, to satisfy current experimental data. Clearly there are some extended regions of contour lines, known as *flat directions*, where the Wilson coefficients attain arbitrarily large values.

These flat directions in the above figure, can be understood by looking at the leading order running and matching conditions between SMEFT and LEFT operators. Following Eqn.-10 we find that for the left-handed vector quark current operators, the  $K_L^0 \rightarrow e^\pm \mu^\mp$  process is proportional

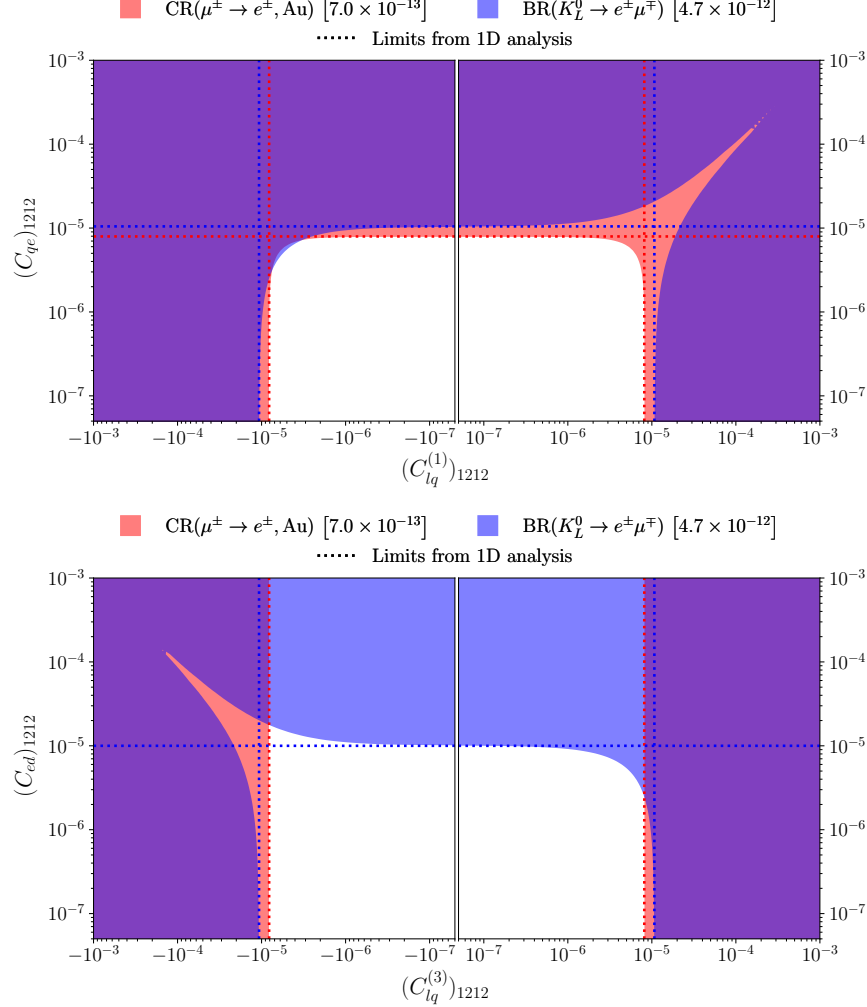


FIG. 13: Limits on 2D WC parameter space from two of the most constraining observables. The allowed region (white) is close to a rectangle determined by 1D limits.

to the square of  $|C_{eu(d)}^{V,LL}|$  and  $|C_{eu(d)}^{V,LR}|$  which can be expressed in terms of SMEFT operators at the matching scale  $\mu = m_Z$  following the relations in Appendix A. Therefore the branching ratio (BR) can be expressed as

$$\text{BR}(K_L^0 \rightarrow e^\pm \mu^\mp) \propto [\mathcal{C}_{\ell q}^{(1)}]_{1212} + [\mathcal{C}_{qe}]_{1212}, \quad (28)$$

where a flat direction in the right panel is obvious for a vanishing  $K_L^0 \rightarrow e^\pm \mu^\mp$ . Similarly, for the situation where operators with vector quark current of both chiralities are present, the same branching ratio is proportional to the square of  $|C_{eu(d)}^{V,LL}|$ ,  $|C_{eu(d)}^{V,RR}|$  and  $|C_{u(d)e}^{V,LR}|$ . Thus for the specific pair,  $\mathcal{C}_{\ell q}^{(3)}$  and  $\mathcal{C}_{ed}$ , the BR can be expressed as

$$\text{BR}(K_L^0 \rightarrow e^\pm \mu^\mp) \propto -[\mathcal{C}_{\ell q}^{(3)}]_{1212} + [\mathcal{C}_{ed}]_{1212}, \quad (29)$$

where the relative sign difference between the WCs to be noted. This is why this flat direction is appearing in the left panel, which is opposite to the same that of the  $\mathcal{C}_{\ell q}^{(1)} - \mathcal{C}_{qe}$  pair.

Similarly, we can find other pairs of WCs with flat directions, which is clearly due to the interplay of RGE matching and running, but it must be noted that the results obtained from these 2-D analyses are consistent with the findings of our 1-D analysis.

## VII. Conclusion

In this paper, we have considered a comprehensive list of low-energy LFV observables which are directly dependent on LFV  $2q2\ell$  operators. Based on the fermion constituents of these processes we have categorized the WCs of these operators by their specific indices in Tables IX-XI and found constraints on each of them coming from all observables. In order to do so, we have implemented several LFV decay modes in the open-source package *Flavio* for the first time, the details of which are provided in sec-IV. The main findings of this analysis, which was done by assuming the presence of only a single operator at  $\Lambda$ , can be summarized as follows.

- We have found that in the  $\mu$ - $e$  sector, almost all the WCs of vector operators consisting of left-handed quark doublet current ( $\mathcal{C}_{\ell q}^{(1)}, \mathcal{C}_{\ell q}^{(3)}$  and  $\mathcal{C}_{qe}$ ) are constrained by most of the observables involving interaction of  $d$ -type quarks. This is because of the convention used in *Warsaw*  $up$  basis in *Wilson* where the running mass matrix of  $u_L$ -type quarks is considered as diagonal at  $\Lambda$ . As a result WCs of operators with  $d_L$ -type operators require CKM rotation and subsequent enhancement due to the CKM matrix elements becomes significant for  $d_L$  and  $s_L$  quarks. On the other hand, observables with  $u$  and  $c$  quarks (quarkonium and LFVDDs) or WCs of the operators with right-handed quark current ( $\mathcal{C}_{ld}, \mathcal{C}_{ed}, \mathcal{C}_{lu}$  and  $\mathcal{C}_{eu}$ ) do not require such a large CKM rotation are thus not constrained or weakly constrained by the observables with different quark FCNC.
- The coefficient  $\mathcal{C}_{1211}$  for all the vector LFV  $2q2\ell$  operators, except  $\mathcal{C}_{\ell q}^{(3)}$ , receive stringent constraint ( $\sim 10^{-6}$ ) from  $\text{CR}(\mu \rightarrow e)$  experiment due to its high precision value.  $[\mathcal{C}_{\ell q}^{(3)}]_{1211}$  is relatively less constrained due to the equal and opposite contribution of SMEFT operators to LEFT operators,  $[\mathcal{C}_{eu}^{V,LL}]_{1211}$  and  $[\mathcal{C}_{ed}^{V,LL}]_{1211}$ , resulting a destructive interference between the proton and neutron contributions to the total amplitude.
- Similarly, other two diagonal coefficients  $[\mathcal{C}]_{1222}$  and  $[\mathcal{C}]_{1233}$  of operators with left-handed quark current, also receive strongest constraints,  $\sim 10^{-4}$  and  $\sim 10^{-3}$  respectively, from the  $\text{CR}(\mu \rightarrow e)$  experiment.
- Although  $J/\psi$  LFV decay has a strong experimental bound ( $\sim 10^{-9}$ ), it generates very weak bound for the coefficient  $[\mathcal{C}]_{1222}$  (relevant for its LFV decay) because of this small lifetime ( $\tau \lesssim 10^{-20}$  s).
- LFVKDs turn out to be the provider of the most stringent constraint ( $\sim 10^{-5}$ ) for the 1212 coefficient of right-handed  $d$ -type quark current operators,  $\mathcal{C}_{ld}$  and  $\mathcal{C}_{ed}$ .
- The coefficients  $\mathcal{C}_{1223}$  ( $\mathcal{C}_{2312}$  for  $\mathcal{C}_{qe}$ ) and  $\mathcal{C}_{1232}$  ( $\mathcal{C}_{2321}$  for  $\mathcal{C}_{qe}$ ) are constrained by LFVBD processes  $B^0 \rightarrow K^{*0} e^- \mu^+$  and  $B^0 \rightarrow K^{*0} e^+ \mu^-$  respectively with limit  $\sim 10^{-3}$ .
- The process  $K_L^0 \rightarrow e^\pm \mu^\mp$  provides strongest constraints for several coefficients ( $[\mathcal{C}]_{1212}, [\mathcal{C}]_{1213}$  and  $[\mathcal{C}]_{1222}$ ) of the scalar operator  $\mathcal{C}_{\ell edq}$ . Likewise  $[\mathcal{C}]_{1231}, [\mathcal{C}]_{1232}$  and  $[\mathcal{C}]_{1233}$  receive strongest constraints from several LFVBD processes.



- For the tensor operator coefficient  $[\mathcal{C}_{\ell equ}^{(3)}]_{1233}$  (or 2133) a strong constraint ( $\sim 10^{-7}$ ) comes from  $\text{CR}(\mu \rightarrow e)$  through leptonic dipole operators. Whereas the coefficient  $[\mathcal{C}_{\ell equ}^{(3)}]_{1221}$  (or 1212, 2121, 2112) can be probed in LFVDDs.
- $\text{CR}(\mu \rightarrow e)$  is the most sensitive process for most of the diagonal elements of vector operators,  $([\mathcal{O}]_{1211,1222,1233})$ , ranging from  $10^4 - 10^6$  GeV irrespective of the chirality. Whereas several LFVBD processes are most sensitive in probing at  $\sim 10^3 - 10^5$  GeV for the coefficients 1213, 1223 (or 1312, 2312) for all left-handed and  $d$ -type right-handed quark current operators. Also, except  $[\mathcal{O}]_{1222}$  for  $J/\Psi$  or  $[\mathcal{O}]_{1233}$  for  $\Upsilon(1S)$ , LFVQDs are found to be least sensitive to other operators and coefficients. For LFVDD processes, they can probe the  $[\mathcal{O}]_{1212}$  coefficients of right-handed  $u$ -type quark-current operators  $\sim 10^3$  GeV, but their chiral counterparts are dominated by  $\text{CR}(\mu \rightarrow e)$ .
- Clearly, compared to  $\mu$ - $e$  sector,  $\tau$ - $\ell$  sector is more promising for vector LFV  $2q2\ell$  operators as the relevant WCs are significantly less constrained ( $\mathcal{C}_{\text{max}} \sim 10^{-4}$ ) and thus can be probed within the energy limit of  $10^4$  GeV.
- When the NP effects are not assumed to be produced by a single SMEFT operator at  $\Lambda$ , cancellations are possible among different contributing elements to the LFV decay rates, resulting in the so-called *flat directions*.

### Acknowledgment

The computations in this project were partially supported by SAMKHYA, the high-performance computing (HPC) facility provided by the Institute of Physics, Bhubaneswar (IOPB). The authors thank Subhadip Bisal for valuable discussions.

### A. Matching between LEFT and SMEFT basis

At the matching scale, the tree-level matching relations between WCs of the  $2q2\ell$  operators in LEFT ( $\mathcal{C}$ ) and those in SMEFT ( $\mathcal{C}$ ) are given by [82]:

$$C_{eu(d)}^{V,LL} = \frac{v^2}{\Lambda^2} \left[ \mathcal{C}_{\alpha\beta ij}^{(1)\ell q} \mp \mathcal{C}_{\alpha\beta ij}^{(3)\ell q} \right] - \frac{\bar{g}_Z^2 v^2}{m_Z^2} [Z_{eL}]_{\alpha\beta} [Z_{u(d)L}]_{ij}, \quad C_{eu(d)}^{V,RR} = \frac{v^2}{\Lambda^2} \left[ \mathcal{C}_{\alpha\beta ij}^{eu(d)} \right] - \frac{\bar{g}_Z^2 v^2}{M_Z^2} [Z_{eR}]_{\alpha\beta} [Z_{u(d)R}]_{ij}, \quad (\text{A1})$$

$$C_{eu(d)}^{V,LR} = \frac{v^2}{\Lambda^2} \left[ \mathcal{C}_{\alpha\beta ij}^{\ell u(d)} \right] - \frac{\bar{g}_Z^2 v^2}{M_Z^2} [Z_{eL}]_{\alpha\beta} [Z_{u(d)R}]_{ij}, \quad C_{u(d)e}^{V,LR} = \frac{v^2}{\Lambda^2} \left[ \mathcal{C}_{ij\alpha\beta}^{qe} \right] - \frac{\bar{g}_Z^2 v^2}{M_Z^2} [Z_{u(d)L}]_{ij} [Z_{eR}]_{\alpha\beta}, \quad (\text{A2})$$

$$C_{eu}^{S,RL} = 0, \quad C_{ed}^{S,RL} = \frac{v^2}{\Lambda^2} \mathcal{C}_{\alpha\beta ij}^{\ell edq}, \quad (\text{A3})$$

$$C_{eu}^{S,RR} = -\frac{v^2}{\Lambda^2} \mathcal{C}_{\alpha\beta ij}^{(1)\ell equ}, \quad C_{ed}^{S,RR} = 0, \quad (\text{A4})$$

$$C_{eu}^{S,LL} = -\frac{v^2}{\Lambda^2} \mathcal{C}_{\beta\alpha ji}^{(1)*\ell equ}, \quad C_{ed}^{S,LL} = 0, \quad (\text{A5})$$

$$C_{eu}^{T,RR} = -\frac{v^2}{\Lambda^2} \mathcal{C}_{\alpha\beta ij}^{(3)\ell equ}, \quad C_{ed}^{T,RR} = 0, \quad (\text{A6})$$

where, in the first equation,  $(-)$  sign between  $\mathcal{C}_{lq}^{(1)}$  and  $\mathcal{C}_{lq}^{(3)}$  is for  $C_{eu}$  and  $(+)$  is for  $C_{ed}$ .  $Z_{ij(\alpha\beta)}$ , with  $i, j(\alpha, \beta)$  being quark(lepton) flavour indices, represents the  $Z$ -boson coupling of the neutral currents in the SMEFT operators. These couplings are given as:

$$[Z_{eL}]_{\alpha\beta} = \left[ \delta_{\alpha\beta} \left( -\frac{1}{2} + \bar{s}^2 \right) - \frac{1}{2} \frac{v_T^2}{\Lambda^2} \left( \mathcal{C}_{H\ell}^{(1)} + \mathcal{C}_{H\ell}^{(3)} \right)_{\alpha\beta} \right] \quad (\text{A7})$$

$$[Z_{eR}]_{\alpha\beta} = \left[ \delta_{\alpha\beta} (+\bar{s}^2) - \frac{1}{2} \frac{v_T^2}{\Lambda^2} \mathcal{C}_{He}^{(1)} \right]_{\alpha\beta} \quad (\text{A8})$$

$$[Z_{uL}]_{ij} = \left[ \delta_{ij} \left( \frac{1}{2} - \frac{2}{3} \bar{s}^2 \right) - \frac{1}{2} \frac{v_T^2}{\Lambda^2} \left( \mathcal{C}_{Hq}^{(1)} - \mathcal{C}_{Hq}^{(3)} \right)_{ij} \right] \quad (\text{A9})$$

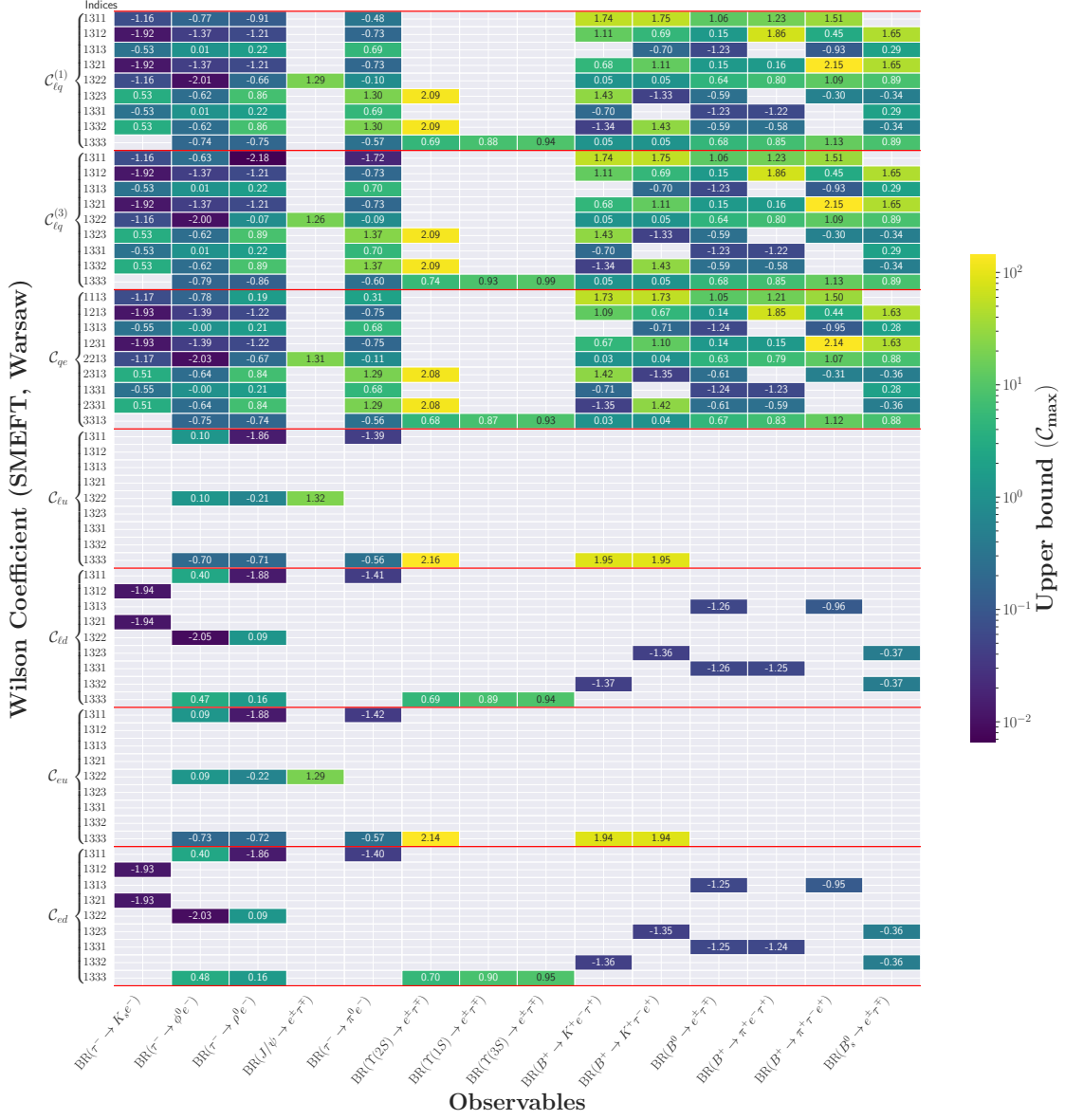
$$[Z_{dL}]_{ij} = \left[ \delta_{ij} \left( -\frac{1}{2} + \frac{1}{3} \bar{s}^2 \right) - \frac{1}{2} \frac{v_T^2}{\Lambda^2} \left( \mathcal{C}_{Hq}^{(1)} + \mathcal{C}_{Hq}^{(3)} \right)_{ij} \right], \quad (\text{A10})$$

$$[Z_{uR}]_{ij} = \left[ \delta_{ij} \left( -\frac{2}{3} \bar{s}^2 \right) - \frac{1}{2} \frac{v_T^2}{\Lambda^2} (\mathcal{C}_{Hu})_{ij} \right] \quad (\text{A11})$$

$$[Z_{dR}]_{ij} = \left[ \delta_{ij} \left( \frac{1}{3} \bar{s}^2 \right) - \frac{1}{2} \frac{v_T^2}{\Lambda^2} (\mathcal{C}_{Hd})_{ij} \right] \quad (\text{A12})$$

Here  $\bar{s} = \sin \bar{\theta}_W$ ,  $\bar{\theta}_W$  being the modified electroweak mixing angle,  $v_T$  is the modified Higgs vacuum expectation value (vev) and  $\mathcal{C}_{Hf}^{(1)/(3)}$  are the associated WC of dimension-6 Higgs-fermion operators. These modifications in the SM values of the parameters arise from the modified electroweak symmetry breaking due to the presence of additional dimension-6 Higgs self-interaction operators in SMEFT, as discussed in Refs. [82, 85].

## B. $\tau - e$ Results



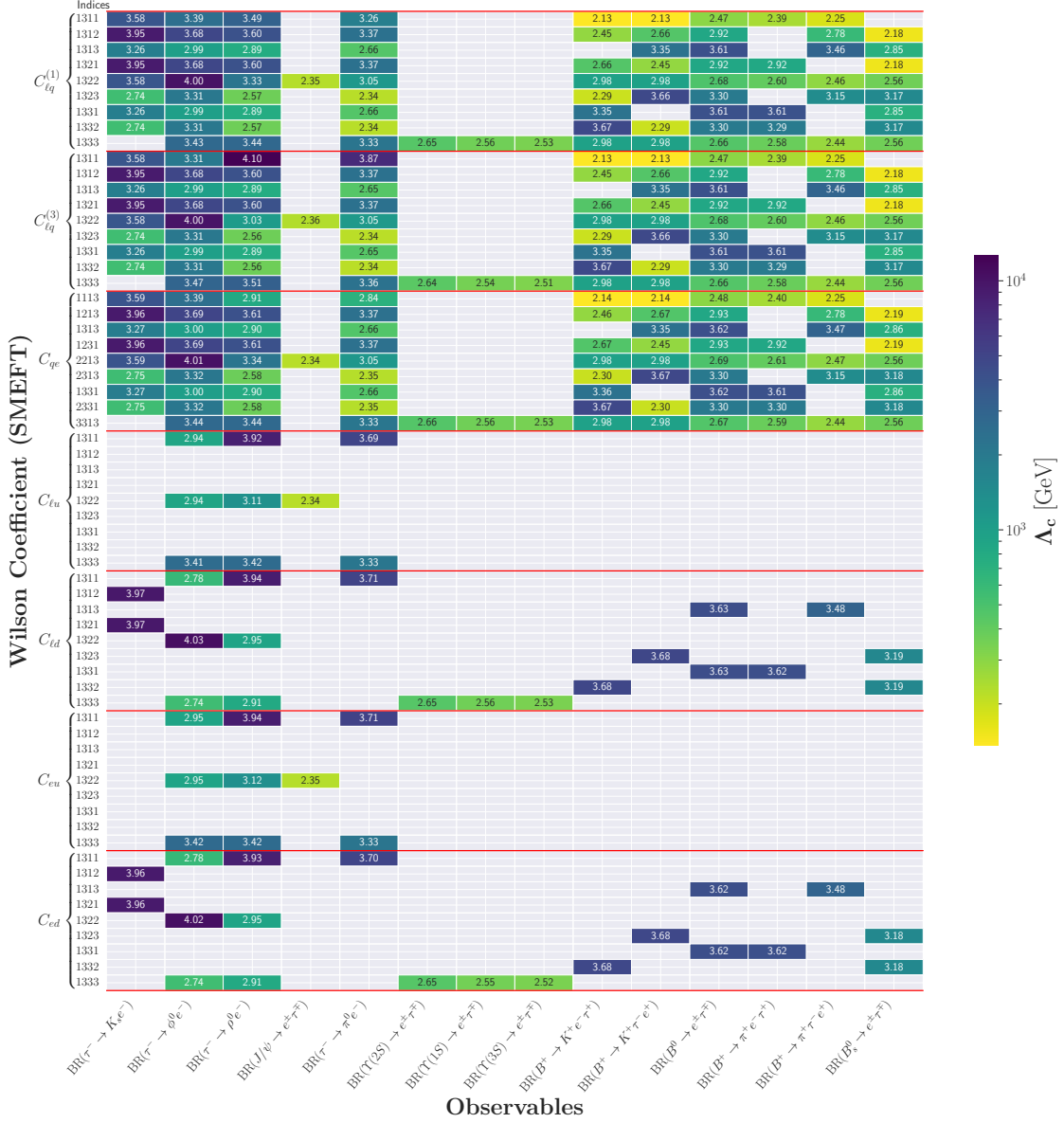
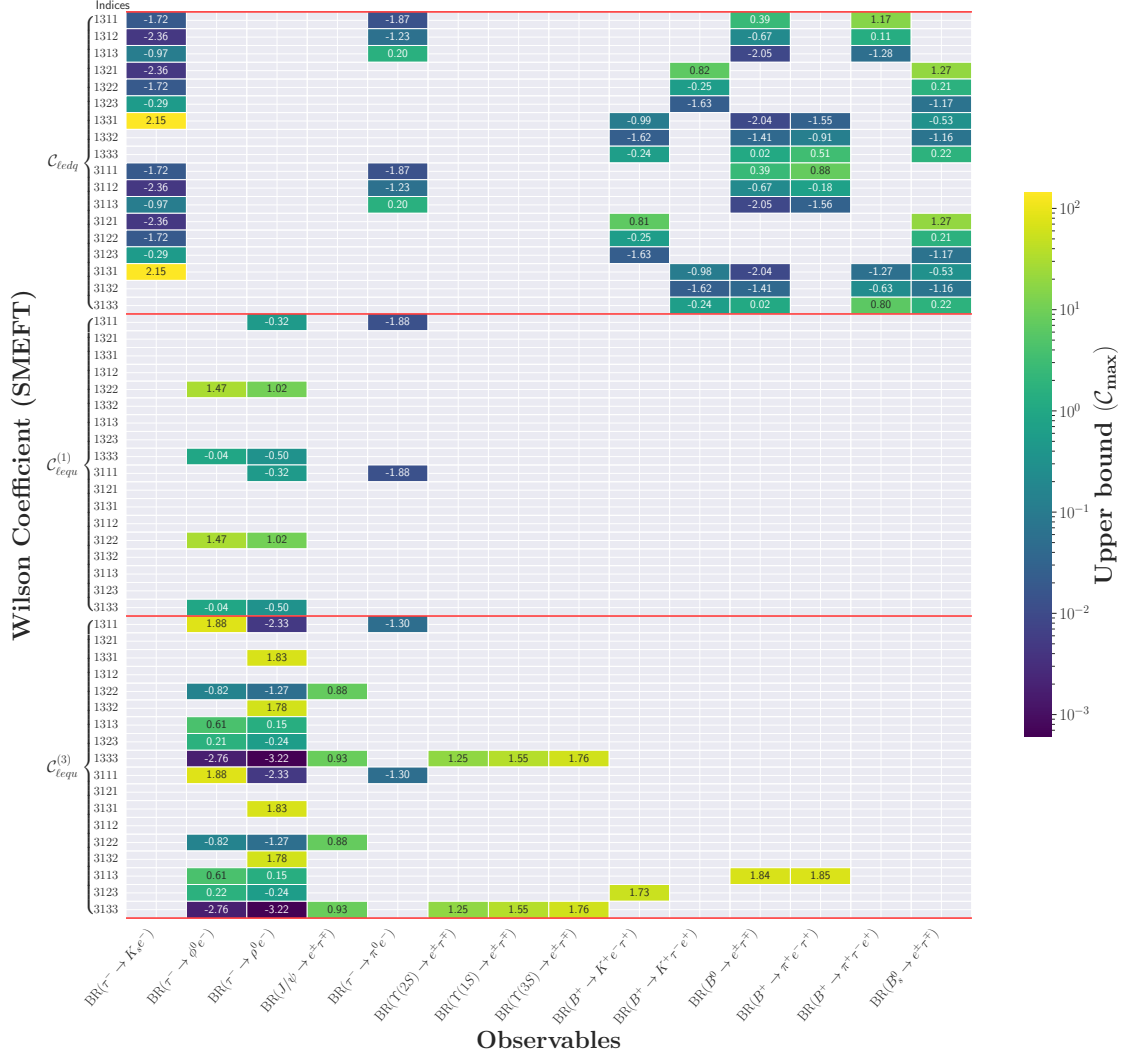


FIG. 15: Same as Fig. 7 but with observables and operators with first- and third-generation charged leptons ( $e^\pm, \tau^\pm$ ).

FIG. 16: Same as Fig. 14 but with scalar and tensor  $2q2\ell$  operators.

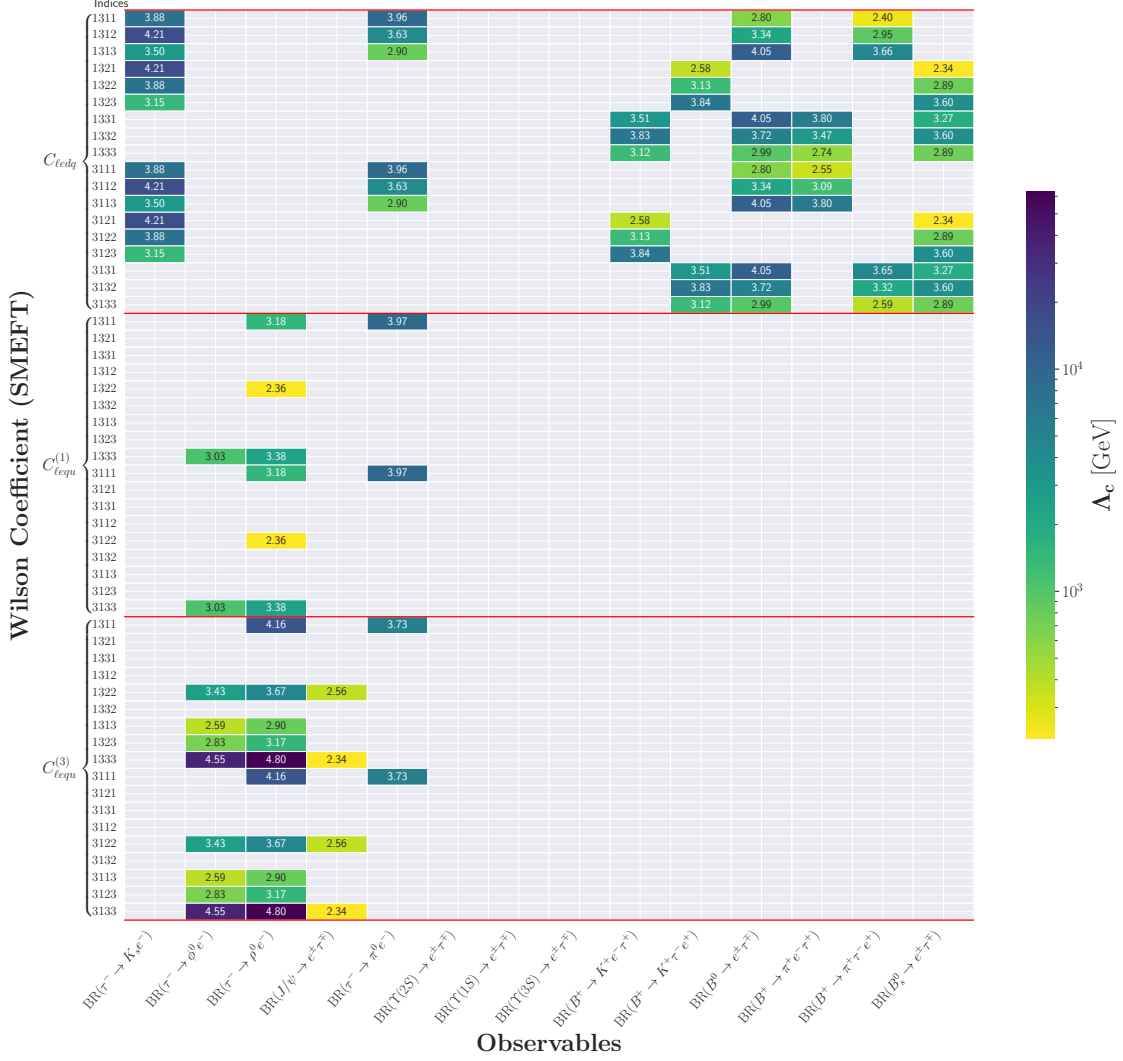


FIG. 17: Same as Fig. 15 but with scalar and tensor operators.

- 
- [1] M. E. Peskin and D. V. Schroeder, *An Introduction to quantum field theory*. Addison-Wesley, Reading, USA, 1995.
  - [2] S. Myers and E. Picasso, *The Design, construction and commissioning of the CERN Large Electron Positron collider*, *Contemp. Phys.* **31** (1990) 387–403.
  - [3] R. R. Wilson, *The Tevatron*, *Phys. Today* **30N10** (1977) 23–30.
  - [4] *LHC Machine*, *JINST* **3** (2008) S08001.
  - [5] ATLAS collaboration, G. Aad et al., *Observation of a new particle in the search for the Standard Model Higgs boson with the ATLAS detector at the LHC*, *Phys. Lett. B* **716** (2012) 1–29, [[1207.7214](#)].
  - [6] A. Crivellin and B. Mellado, *Anomalies in Particle Physics*, [2309.03870](#).
  - [7] H. Georgi, *Effective field theory*, *Ann. Rev. Nucl. Part. Sci.* **43** (1993) 209–252.
  - [8] W. Buchmuller and D. Wyler, *Effective Lagrangian Analysis of New Interactions and Flavor Conservation*, *Nucl. Phys. B* **268** (1986) 621–653.
  - [9] P. Bechtle, C. Chall, M. King, M. Kraemer, P. Maettig and M. Stöltzner, *Bottoms Up: Standard Model Effective Field Theory from a Model Perspective*, [2201.08819](#).

- [10] B. Grzadkowski, M. Iskrzynski, M. Misiak and J. Rosiek, *Dimension-Six Terms in the Standard Model Lagrangian*, *JHEP* **10** (2010) 085, [[1008.4884](#)].
- [11] S. Davidson, Y. Kuno and M. Yamanaka, *Selecting  $\mu \rightarrow e$  conversion targets to distinguish lepton flavour-changing operators*, *Phys. Lett. B* **790** (2019) 380–388, [[1810.01884](#)].
- [12] A. Crivellin, S. Davidson, G. M. Pruna and A. Signer, *Renormalisation-group improved analysis of  $\mu \rightarrow e$  processes in a systematic effective-field-theory approach*, *JHEP* **05** (2017) 117, [[1702.03020](#)].
- [13] V. Cirigliano, S. Davidson and Y. Kuno, *Spin-dependent  $\mu \rightarrow e$  conversion*, *Phys. Lett. B* **771** (2017) 242–246, [[1703.02057](#)].
- [14] S. Davidson, Y. Kuno and A. Saporta, “*Spin-dependent*”  $\mu \rightarrow e$  conversion on light nuclei, *Eur. Phys. J. C* **78** (2018) 109, [[1710.06787](#)].
- [15] S. Davidson, Y. Kuno, Y. Uesaka and M. Yamanaka, *Probing  $\mu e \gamma \gamma$  contact interactions with  $\mu \rightarrow e$  conversion*, *Phys. Rev. D* **102** (2020) 115043, [[2007.09612](#)].
- [16] S. Davidson, *Completeness and complementarity for  $\mu \rightarrow e \gamma \mu \rightarrow e \bar{e} e$  and  $\mu A \rightarrow e A$* , *JHEP* **02** (2021) 172, [[2010.00317](#)].
- [17] V. Cirigliano, K. Fuyuto, C. Lee, E. Mereghetti and B. Yan, *Charged Lepton Flavor Violation at the EIC*, *JHEP* **03** (2021) 256, [[2102.06176](#)].
- [18] J. Kumar, *Renormalization group improved implications of semileptonic operators in SMEFT*, *JHEP* **01** (2022) 107, [[2107.13005](#)].
- [19] A. Crivellin, S. Najjari and J. Rosiek, *Lepton Flavor Violation in the Standard Model with general Dimension-Six Operators*, *JHEP* **04** (2014) 167, [[1312.0634](#)].
- [20] G. M. Pruna and A. Signer, *The  $\mu \rightarrow e \gamma$  decay in a systematic effective field theory approach with dimension 6 operators*, *JHEP* **10** (2014) 014, [[1408.3565](#)].
- [21] R. Alonso, B. Grinstein and J. Martin Camalich,  *$SU(2) \times U(1)$  gauge invariance and the shape of new physics in rare  $B$  decays*, *Phys. Rev. Lett.* **113** (2014) 241802, [[1407.7044](#)].
- [22] J. Aebischer, A. Crivellin, M. Fael and C. Greub, *Matching of gauge invariant dimension-six operators for  $b \rightarrow s$  and  $b \rightarrow c$  transitions*, *JHEP* **05** (2016) 037, [[1512.02830](#)].
- [23] A. Crivellin, L. Hofer, J. Matias, U. Nierste, S. Pokorski and J. Rosiek, *Lepton-flavour violating  $B$  decays in generic  $Z'$  models*, *Phys. Rev. D* **92** (2015) 054013, [[1504.07928](#)].
- [24] D. Bećirević, O. Sumensari and R. Zukanovich Funchal, *Lepton flavor violation in exclusive  $b \rightarrow s$  decays*, *Eur. Phys. J. C* **76** (2016) 134, [[1602.00881](#)].
- [25] S. Descotes-Genon, D. A. Faroughy, I. Plakias and O. Sumensari, *Probing lepton flavor violation in meson decays with LHC data*, *Eur. Phys. J. C* **83** (2023) 753, [[2303.07521](#)].
- [26] M. I. Ali, U. Chattopadhyay, N. Rajeev and J. Roy, *SMEFT analysis of charged lepton flavor violating  $B$ -meson decays*, *Phys. Rev. D* **109** (2024) 075028, [[2312.05071](#)].
- [27] L. Calibbi, X. Marcano and J. Roy,  *$Z$  lepton flavour violation as a probe for new physics at future  $e^+e^-$  colliders*, *Eur. Phys. J. C* **81** (2021) 1054, [[2107.10273](#)].
- [28] J. M. Cullen and B. D. Pecjak, *Higgs decay to fermion pairs at NLO in SMEFT*, *JHEP* **11** (2020) 079, [[2007.15238](#)].
- [29] L. Calibbi, T. Li, X. Marcano and M. A. Schmidt, *Indirect constraints on lepton-flavor-violating quarkonium decays*, *Phys. Rev. D* **106** (2022) 115039, [[2207.10913](#)].
- [30] BELLE collaboration, T. Ohshima, *Study of LFV in tau decay at Belle*, *Nucl. Phys. B Proc. Suppl.* **169** (2007) 174–185.
- [31] BELLE-II collaboration, L. Aggarwal et al., *Snowmass White Paper: Belle II physics reach and plans for the next decade and beyond*, [2207.06307](#).
- [32] BABAR collaboration, B. Aubert et al., *Search for Lepton Flavor Violating Decays  $\tau^\pm \rightarrow \ell^\pm \pi^0, \ell^\pm \eta, \ell^\pm \eta'$* , *Phys. Rev. Lett.* **98** (2007) 061803, [[hep-ex/0610067](#)].
- [33] BELLE-II collaboration, W. Altmannshofer et al., *The Belle II Physics Book*, *PTEP* **2019** (2019) 123C01, [[1808.10567](#)]. [Erratum: PTEP 2020, 029201 (2020)].
- [34] BELLE collaboration, N. Tsuzuki et al., *Search for lepton-flavor-violating  $\tau$  decays into a lepton and a vector meson using the full Belle data sample*, *JHEP* **06** (2023) 118, [[2301.03768](#)].
- [35] BELLE-II, BELLE collaboration, I. Adachi et al., *Search for lepton-flavor-violating  $\tau^- \rightarrow \ell^- K_s^0$  decays at Belle and Belle II*, [2504.15745](#).
- [36] SINDRUM II collaboration, W. H. Bertl et al., *A Search for muon to electron conversion in muonic gold*, *Eur. Phys. J. C* **47** (2006) 337–346.
- [37] P. Wintz, *Results of the SINDRUM-II experiment*, *Conf. Proc. C* **980420** (1998) 534–546.



- [38] Mu2E collaboration, L. Bartoszek et al., *Mu2e Technical Design Report*, [1501.05241](#).
- [39] COMET collaboration, Y. Kuno, *A search for muon-to-electron conversion at J-PARC: The COMET experiment*, *PTEP* **2013** (2013) 022C01.
- [40] COMET collaboration, R. Abramishvili et al., *COMET Phase-I Technical Design Report*, *PTEP* **2020** (2020) 033C01, [[1812.09018](#)].
- [41] BESIII collaboration, M. Ablikim et al., *Search for the lepton flavor violating decay  $J/\psi \rightarrow e\mu$* , *Sci. China Phys. Mech. Astron.* **66** (2023) 221011, [[2206.13956](#)].
- [42] BESIII collaboration, M. Ablikim et al., *Search for the charged lepton flavor violating decay  $J/\psi \rightarrow e\tau$* , *Phys. Rev. D* **103** (2021) 112007, [[2103.11540](#)].
- [43] BES collaboration, M. Ablikim et al., *Search for the lepton flavor violation processes  $J/\psi \rightarrow \mu\tau$  and  $e\tau$* , *Phys. Lett. B* **598** (2004) 172–177, [[hep-ex/0406018](#)].
- [44] BELLE collaboration, S. Patra et al., *Search for charged lepton flavor violating decays of  $\Upsilon(1S)$* , *JHEP* **05** (2022) 095, [[2201.09620](#)].
- [45] BELLE collaboration, R. Dhamija et al., *Search for charged-lepton flavor violation in  $\Upsilon(2S) \rightarrow \ell^\mp \tau^\pm$  ( $\ell = e, \mu$ ) decays at Belle*, *JHEP* **02** (2024) 187, [[2309.02739](#)].
- [46] BABAR collaboration, J. P. Lees et al., *Search for Lepton Flavor Violation in  $\Upsilon(3S) \rightarrow e^\pm \mu^\mp$* , *Phys. Rev. Lett.* **128** (2022) 091804, [[2109.03364](#)].
- [47] BABAR collaboration, J. P. Lees et al., *Search for Charged Lepton Flavor Violation in Narrow Upsilon Decays*, *Phys. Rev. Lett.* **104** (2010) 151802, [[1001.1883](#)].
- [48] NA62 collaboration, E. Cortina Gil et al., *Search for Lepton Number and Flavor Violation in  $K^+$  and  $\pi^0$  Decays*, *Phys. Rev. Lett.* **127** (2021) 131802, [[2105.06759](#)].
- [49] R. Appel et al., *An Improved limit on the rate of decay  $K^+ \rightarrow \pi^+ \mu^+ e^-$* , *Phys. Rev. Lett.* **85** (2000) 2450–2453, [[hep-ex/0005016](#)].
- [50] KTeV collaboration, E. Abouzaid et al., *Search for lepton flavor violating decays of the neutral kaon*, *Phys. Rev. Lett.* **100** (2008) 131803, [[0711.3472](#)].
- [51] D. B. White et al., *Search for the decays  $\eta \rightarrow \mu e$  and  $\eta \rightarrow e e$* , *Phys. Rev. D* **53** (1996) 6658–6661.
- [52] CLEO collaboration, R. A. Briere et al., *Rare decays of the eta-prime*, *Phys. Rev. Lett.* **84** (2000) 26–30, [[hep-ex/9907046](#)].
- [53] REDTOP collaboration, J. Elam et al., *The REDTOP experiment: Rare  $\eta/\eta'$  Decays To Probe New Physics*, [2203.07651](#).
- [54] BNL collaboration, D. Ambrose et al., *New limit on muon and electron lepton number violation from  $K0(L) \rightarrow \mu^\pm e^\mp$  decay*, *Phys. Rev. Lett.* **81** (1998) 5734–5737, [[hep-ex/9811038](#)].
- [55] A. Sher et al., *An Improved upper limit on the decay  $K^+ \rightarrow \pi^+ \mu^+ e^-$* , *Phys. Rev. D* **72** (2005) 012005, [[hep-ex/0502020](#)].
- [56] PARTICLE DATA GROUP collaboration, P. A. Zyla et al., *Review of Particle Physics*, *PTEP* **2020** (2020) 083C01.
- [57] BABAR collaboration, J. P. Lees et al., *Search for lepton-flavor-violating decays  $D^0 \rightarrow X^0 e^\pm \mu^\mp$* , *Phys. Rev. D* **101** (2020) 112003, [[2004.09457](#)].
- [58] LHCb collaboration, R. Aaij et al., *Searches for 25 rare and forbidden decays of  $D^+$  and  $D_s^+$  mesons*, *JHEP* **06** (2021) 044, [[2011.00217](#)].
- [59] LHCb collaboration, R. Aaij et al., *Search for Lepton-Flavor Violating Decays  $B^+ \rightarrow K^+ \mu^\pm e^\mp$* , *Phys. Rev. Lett.* **123** (2019) 241802, [[1909.01010](#)].
- [60] LHCb collaboration, *Search for the lepton-flavour violating decays  $B^0 \rightarrow K^{*0} \mu^\pm e^\mp$  and  $B_s^0 \rightarrow \phi \mu^\pm e^\mp$* , [2207.04005](#).
- [61] BABAR collaboration, B. Aubert et al., *Search for the rare decay  $B \rightarrow \pi l^+ l^-$* , *Phys. Rev. Lett.* **99** (2007) 051801, [[hep-ex/0703018](#)].
- [62] LHCb collaboration, R. Aaij et al., *Search for the lepton-flavour violating decays  $B_{(s)}^0 \rightarrow e^\pm \mu^\mp$* , *JHEP* **03** (2018) 078, [[1710.04111](#)].
- [63] LHCb collaboration, R. Aaij et al., *Physics case for an LHCb Upgrade II - Opportunities in flavour physics, and beyond, in the HL-LHC era*, [1808.08865](#).
- [64] BELLE collaboration, S. Watanuki et al., *Search for the Lepton Flavor Violating Decays  $B \rightarrow K + \tau \pm \ell^\mp$  ( $\ell = e, \mu$ ) at Belle*, *Phys. Rev. Lett.* **130** (2023) 261802, [[2212.04128](#)].
- [65] LHCb collaboration, *Search for the lepton-flavour violating decays  $B^0 \rightarrow K^{*0} \tau^\pm \mu^\mp$* , [2209.09846](#).

- [66] BABAR collaboration, J. P. Lees et al., *A search for the decay modes  $B^{+-} \rightarrow h^{+-}\tau^{+-}l$* , *Phys. Rev. D* **86** (2012) 012004, [[1204.2852](#)].
- [67] LHCb collaboration, R. Aaij et al., *Search for the lepton-flavor violating decay  $Bs0 \rightarrow \phi\mu\pm\tau\mp$* , *Phys. Rev. D* **110** (2024) 072014, [[2405.13103](#)].
- [68] BELLE collaboration, H. Atmacan et al., *Search for  $B^0 \rightarrow \tau^\pm\ell^\mp$  ( $\ell = e, \mu$ ) with a hadronic tagging method at Belle*, *Phys. Rev. D* **104** (2021) L091105, [[2108.11649](#)].
- [69] LHCb collaboration, R. Aaij et al., *Search for the lepton-flavour-violating decays  $B_s^0 \rightarrow \tau^\pm\mu^\mp$  and  $B^0 \rightarrow \tau^\pm\mu^\mp$* , *Phys. Rev. Lett.* **123** (2019) 211801, [[1905.06614](#)].
- [70] BELLE collaboration, L. Nayak et al., *Search for  $B_s^0 \rightarrow \ell^\mp\tau^\pm$  with the Semi-leptonic Tagging Method at Belle*, *JHEP* **08** (2023) 178, [[2301.10989](#)].
- [71] D. E. Hazard and A. A. Petrov, *Radiative lepton flavor violating B, D, and K decays*, *Phys. Rev. D* **98** (2018) 015027, [[1711.05314](#)].
- [72] A. F. Zarnecki, *Global analysis of eeqq contact interactions and future prospects for high-energy physics*, *Eur. Phys. J. C* **11** (1999) 539–557, [[hep-ph/9904334](#)].
- [73] A. Ibarra, E. Masso and J. Redondo, *Systematic approach to gauge-invariant relations between lepton flavor violating processes*, *Nucl. Phys. B* **715** (2005) 523–535, [[hep-ph/0410386](#)].
- [74] M. Carpentier and S. Davidson, *Constraints on two-lepton, two quark operators*, *Eur. Phys. J. C* **70** (2010) 1071–1090, [[1008.0280](#)].
- [75] F. Garosi, D. Marzocca, A. R. Sánchez and A. Stanzione, *Indirect constraints on top quark operators from a global SMEFT analysis*, *JHEP* **12** (2023) 129, [[2310.00047](#)].
- [76] E. Fernández-Martínez, X. Marcano and D. Naredo-Tuero, *Global Lepton Flavour Violating Constraints on New Physics*, [2403.09772](#).
- [77] J. de Blas, J. C. Criado, M. Perez-Victoria and J. Santiago, *Effective description of general extensions of the Standard Model: the complete tree-level dictionary*, *JHEP* **03** (2018) 109, [[1711.10391](#)].
- [78] I. Plakias and O. Sumensari, *Lepton Flavor Violation in Semileptonic Observables*, [2312.14070](#).
- [79] U. Chattopadhyay, D. Das and S. Mukherjee, *Probing Lepton Flavor Violating decays in MSSM with Non-Holomorphic Soft Terms*, *JHEP* **06** (2020) 015, [[1911.05543](#)].
- [80] B. De, D. Das, M. Mitra and N. Sahoo, *Magnetic moments of leptons, charged lepton flavor violations and dark matter phenomenology of a minimal radiative Dirac neutrino mass model*, *JHEP* **08** (2022) 202, [[2106.00979](#)].
- [81] E. E. Jenkins, A. V. Manohar and M. Trott, *Renormalization Group Evolution of the Standard Model Dimension Six Operators I: Formalism and lambda Dependence*, *JHEP* **10** (2013) 087, [[1308.2627](#)].
- [82] E. E. Jenkins, A. V. Manohar and M. Trott, *Renormalization Group Evolution of the Standard Model Dimension Six Operators II: Yukawa Dependence*, *JHEP* **01** (2014) 035, [[1310.4838](#)].
- [83] R. Alonso, E. E. Jenkins, A. V. Manohar and M. Trott, *Renormalization Group Evolution of the Standard Model Dimension Six Operators III: Gauge Coupling Dependence and Phenomenology*, *JHEP* **04** (2014) 159, [[1312.2014](#)].
- [84] B. Grinstein, M. J. Savage and M. B. Wise,  *$B \rightarrow X(s) e^+ e^-$  in the Six Quark Model*, *Nucl. Phys. B* **319** (1989) 271–290.
- [85] E. E. Jenkins, A. V. Manohar and P. Stoffer, *Low-Energy Effective Field Theory below the Electroweak Scale: Operators and Matching*, *JHEP* **03** (2018) 016, [[1709.04486](#)].
- [86] E. E. Jenkins, A. V. Manohar and P. Stoffer, *Low-Energy Effective Field Theory below the Electroweak Scale: Anomalous Dimensions*, *JHEP* **01** (2018) 084, [[1711.05270](#)].
- [87] J. Aebischer, J. Kumar and D. M. Straub, *Wilson: a Python package for the running and matching of Wilson coefficients above and below the electroweak scale*, *Eur. Phys. J. C* **78** (2018) 1026, [[1804.05033](#)].
- [88] D. M. Straub, *flavio: a Python package for flavour and precision phenomenology in the Standard Model and beyond*, [1810.08132](#).
- [89] G. Buchalla, A. J. Buras and M. E. Lautenbacher, *Weak decays beyond leading logarithms*, *Rev. Mod. Phys.* **68** (1996) 1125–1144, [[hep-ph/9512380](#)].
- [90] G. Burdman, E. Golowich, J. L. Hewett and S. Pakvasa, *Rare charm decays in the standard model and beyond*, *Phys. Rev. D* **66** (2002) 014009, [[hep-ph/0112235](#)].
- [91] S. de Boer and G. Hiller, *Flavor and new physics opportunities with rare charm decays into leptons*, *Phys. Rev. D* **93** (2016) 074001, [[1510.00311](#)].

- [92] F. J. Gilman and M. B. Wise,  $K \rightarrow \pi e^+ e^-$  in the Six Quark Model, *Phys. Rev. D* **21** (1980) 3150.
- [93] T. Inami and C. S. Lim, *Effects of Superheavy Quarks and Leptons in Low-Energy Weak Processes*  $k(L) \rightarrow \mu \text{ anti-}\mu$ ,  $K^+ \rightarrow \pi^+ \text{ Neutrino anti-neutrino}$  and  $K^0 \leftrightarrow \text{anti-}K^0$ , *Prog. Theor. Phys.* **65** (1981) 297. [Erratum: *Prog.Theor.Phys.* 65, 1772 (1981)].
- [94] C. Dib, I. Dunietz and F. J. Gilman,  $K(L) \rightarrow \pi^0 \text{ Lepton}^+ \text{ Lepton}^- \text{ Decays for Large } m(t)$ , *Phys. Rev. D* **39** (1989) 2639.
- [95] P. Ball and R. Zwicky,  $B_{d,s} \rightarrow \rho, \omega, K^*, \phi$  decay form-factors from light-cone sum rules revisited, *Phys. Rev. D* **71** (2005) 014029, [[hep-ph/0412079](#)].
- [96] A. Khodjamirian, T. Mannel and N. Offen, *Form-factors from light-cone sum rules with B-meson distribution amplitudes*, *Phys. Rev. D* **75** (2007) 054013, [[hep-ph/0611193](#)].
- [97] C.-D. Lu and W. Wang, *Analysis of  $B \rightarrow K_J^*(\rightarrow K\pi)\mu^+\mu^-$  in the higher kaon resonance region*, *Phys. Rev. D* **85** (2012) 034014, [[1111.1513](#)].
- [98] D. E. Hazard and A. A. Petrov, *Lepton flavor violating quarkonium decays*, *Phys. Rev. D* **94** (2016) 074023, [[1607.00815](#)].
- [99] M. Hoferichter, J. Menéndez and F. Noël, *Improved Limits on Lepton-Flavor-Violating Decays of Light Pseudoscalars via Spin-Dependent  $\mu \rightarrow e$  Conversion in Nuclei*, *Phys. Rev. Lett.* **130** (2023) 131902, [[2204.06005](#)].
- [100] A. Crivellin, G. D'Ambrosio, M. Hoferichter and L. C. Tunstall, *Violation of lepton flavor and lepton flavor universality in rare kaon decays*, *Phys. Rev. D* **93** (2016) 074038, [[1601.00970](#)].
- [101] Fayyazuddin, M. J. Aslam and C.-D. Lu, *Lepton Flavor Violating Decays of B and K Mesons in Models with Extended Gauge Group*, *Int. J. Mod. Phys. A* **33** (2018) 1850087, [[1805.00177](#)].
- [102] A. Ryd and A. A. Petrov, *Hadronic D and D(s) Meson Decays*, *Rev. Mod. Phys.* **84** (2012) 65–117, [[0910.1265](#)].
- [103] A. Abada, D. Bečirević, M. Lucente and O. Sumensari, *Lepton flavor violating decays of vector quarkonia and of the Z boson*, *Phys. Rev. D* **91** (2015) 113013, [[1503.04159](#)].
- [104] J. Aebischer, J. Kumar, P. Stangl and D. M. Straub, *A Global Likelihood for Precision Constraints and Flavour Anomalies*, *Eur. Phys. J. C* **79** (2019) 509, [[1810.07698](#)].
- [105] Y. Kuno and Y. Okada, *Muon decay and physics beyond the standard model*, *Rev. Mod. Phys.* **73** (2001) 151–202, [[hep-ph/9909265](#)].
- [106] R. Kitano, M. Koike and Y. Okada, *Detailed calculation of lepton flavor violating muon electron conversion rate for various nuclei*, *Phys. Rev. D* **66** (2002) 096002, [[hep-ph/0203110](#)]. [Erratum: *Phys.Rev.D* 76, 059902 (2007)].